INSTRUMENTAL ANALYSIS OF PASYLATED ASPARAGINASE, JZP-341, A PRE-CLINICAL DRUG CANDIDATE

SHAKIBA GHAFFARI

A THESIS SUBMITTED TO

THE FACULTY OF GRADUATE STUDIES

IN PARTIAL FULFILLMENT OF

THE REQUIREMENTS FOR

THE DEGREE OF MASTER OF SCIENCE

GRADUATE PROGRAM IN CHEMISTRY

YORK UNIVERSITY

TORONTO, ONTARIO

SEPT 2023

Abstract

Bio-betters are second-generation biopharmaceutical drugs that aim to improve the original drug's pharmacokinetic or pharmacodynamic properties through minor physical modifications. Bio-betters require extensive characterization. Here, we investigate: JZP-341, a long-acting asparaginase bio-better used to treat leukemia. JZP-341 has a disordered proline-alanine-serine (PAS) tail that increases the drug's size and thereby its serum half-life. A long serum half-life decreases the dosage frequency, providing more freedom to the patient. We assess the structural heterogeneity, charge heterogeneity, and enzyme kinetics of JZP-341 to better understand the effects of the PAS tail on the drug *via* the methods of capillary electrophoresis (CE), mass spectrometry (MS), and chromatography. We observe size heterogeneity and charge heterogeneity. We also developed a native capillary gel electrophoresis assay and an automated label-free CE-MS enzyme activity assay to study JZP-341. A detailed understanding of the role of PAS tail on JZP-341 requires further assay development and sophisticated equipment.

Acknowledgements

I thank my supervisor, Dr. Sergey N. Krylov, for their mentorship and the opportunity to further my education. I thank my committee members Dr. Derek Wilson and Dr. Ryan Hili for their approachability and support. I thank NSERC, MITACS, and York University for making this research possible.

I thank my dear lab-mates: An Le Thi Hoai, Eden Teclemichael, TongYe Wang, Liang Hu, Jean-Luc Rukundo, Giammarco Nebbioso, Nikita Ivanov, and Stanislav Beloborodov for always being available to train, listen, help, encourage, and make my MSc experience enjoyable.

I thank my family and my husband, Brian, for being with me every step of the way.

Table of Contents

List of Figures

List of Schemes

List of Abbreviations

Ala: Alanine

ALL: Acute lymphoblastic leukemia

Asn: Asparagine

Asp: Aspartic acid

BME: Betamercaptoethanol

BPD: Biopharmaceutical drug

CE: Capillary electrophoresis

CGE: Capillary gel electrophoresis

cIEF: Capillary isoelectric focusing

CZE: Capillary zone electrophoresis

EB: Enzyme buffer

EK: Lysine and glutamine polypeptide chain

FAM: Fluoroscein amidite

IMReSQ: Inject-Mix-React-Separate-Quantitate

JZP-341: Jazz pharmaceuticals pre-clinical pasylated asparaginase

kDa: Kilodalton

LIF: Laser induced fluorescence

MS: Mass spectrometry

MWCO: Molecular weight cut off

OPA: O-phthaldehyde

OPI: Open-port interface

PAS: Proline, alanine, and serine polypeptide chain

PEG: Polyethylene glycol

Pro: Proline

RB: Running buffer

SB: Sample buffer

SDS: Sodium dodecyl sulfate

Ser: Serine

SFI: Sheath-flow interface

UV: Ultraviolet

XTEN: Alanine, glycine, glutamine, proline, serine, threonine polypeptide chain

Chapter 1: Background

1.1 Improvement of Pharmacokinetic Properties of Biopharmaceutical Drugs

Biopharmaceutical drugs (BPD) are complex and highly effective therapeutic tools used against various diseases, including cancers and infections. BPDs include proteins and nucleic acids that are typically administered to patients by injection. BPDs circulate in the body following unique pharmacokinetic principles of absorption, distribution, metabolism, and excretion. Drug excretion is a natural process of removing a medication or a drug metabolite from the body. Protein BPDs are typically catabolized by proteases into smaller peptides and then excreted renally.[1] The rate of renal elimination is directly proportional to the size of the BPD, therefore size is an important pharmacokinetic parameter of BPDs.

A familiar example is insulin for diabetes treatment. Insulin is a 5.8 kDa peptide hormone that promotes the absorption of sugar from the bloodstream. Insulin is one of the earliest and smallest BPDs. Due to its small size, the serum half-life of insulin is five minutes, and most patients require multiple doses to manage their blood sugar.[2] Frequent dosage can be uncomfortable, inconvenient, and increase the risk of infection.[3] To improve the half-life of insulin, a variety of "long-acting" or "second-generation" insulin analogs have been introduced to the market. Second-generation drug are also known as "bio-betters" – a modified original drug with superior pharmacokinetic or pharmacodynamic properties.[4]

1.2 Half-Life Extenders of Biopharmaceutical Drugs

The serum half-life of drugs can be improved by increasing the size of the BPD. The size of a BPD can be chemically or genetically extended by fusion of a large inert moiety onto the protein drug.[5] Witteloostuijn *et al.* summarize the forms of half-life extenders of BPDs to improve the pharmacokinetic properties.[6] The most common BPD extender is polyethylene glycol (PEG). PEG is a disordered polymer that can be chemically fused onto a BPD to extend the size of the

therapeutic. This approach was used extensively for the past 20 years; however, due to the high cost of production, complicated fusion reaction, and new evidence of PEG bioaccumulation within patients, researchers have turned to more natural conjugates.[6,7] Natural extenders include lipid chains, glycans, albumin, Fc domains of antibodies, and polypeptide chains. Reported polypeptide half-life extenders include EKylation (Lys, Glu), XTENlyation (Ala, Gly, Glu, Pro, Ser, Thr), and the focus of this report, PASylation (Pro, Ala, Ser).[8]

1.3 Proline-Alanine-Serine Tails or PASylation

In 2013, Skerra et al. proved that randomly stringed PAS polypeptide chains of 200-6,000 residues form inert random coiled tails that can be synthesized directly on the protein using a modified vector, **Scheme 1A.**[9] PASylated proteins demonstrate high solubility and stability, full bio-functionality *in vitro* and in animal models, high bioavailability, and significantly high serum half-life.[10,11] Since their inception, PASylated proteins have been used to create long-acting growth hormones, multiple sclerosis drugs, cancer treatments, and imaging radiotracers, **Scheme 1B**.[10] So far, PASylated anti-HER2 cancer imaging radiotracer has been successfully used in clinical settings.[12] PASylated drugs must be extensively characterized and compared to their original drug to gain regulatory approval and enter clinical trials. Biophysical PAS characterization methods includes size exclusion chromatography, dynamic light scattering, circular dichroism, and other low-resolution structural determination methods. From the biophysical characterizations, researchers have concluded that the PAS random coil has similar biophysical properties to PEG tails.[10] Moreover, PAS tails have a greater hydrophilicity, greater hydrodynamic volume-to-mass ratio, and lower viscosity than PEG tails, all of which are favourable characteristics for protein drugs.[10]

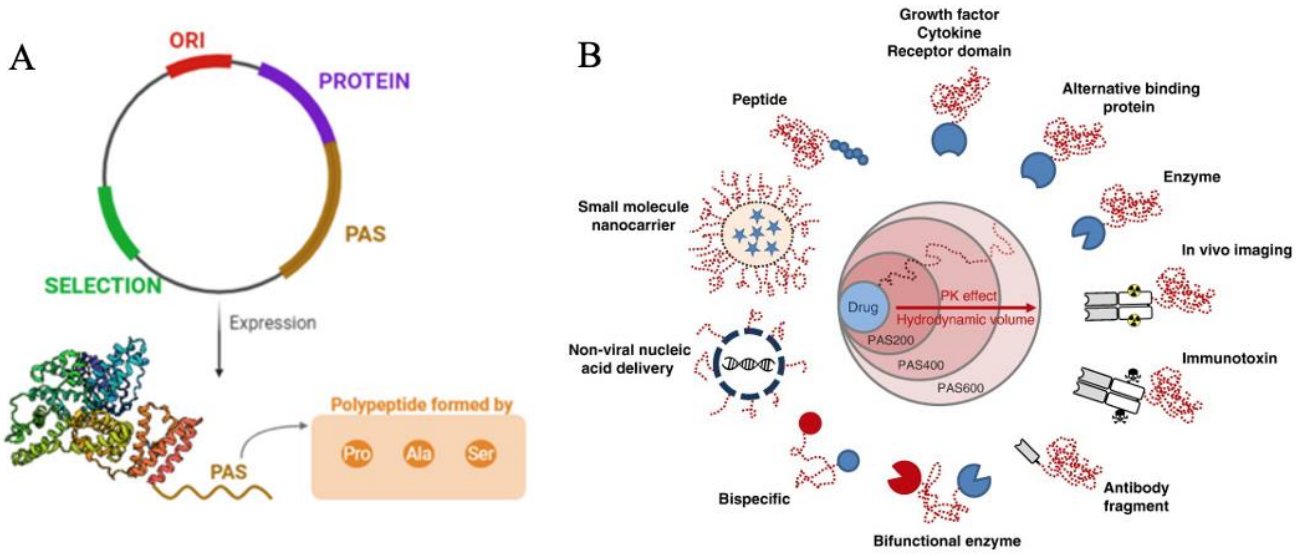

Scheme 1 A Illustration of a generic PASylated protein DNA vector (adapted from Ref. 11) and B- Illustration of PAS tail on a variety of drugs (adapted from Ref 7)

1.4 Challenges associated with analyzing PASylated drugs

Despite the simplicity of the PAS tail, limited high-resolution analysis has been reported. PASylated BPDs are particularly difficult to analyze using common analytical methods due to their intrinsic chemical and structural properties. Specifically, (i) PAS amino acids are not UV active; (ii) PAS amino acids do not bind sodium dodecyl sulfate (SDS); (iii) PAS tails have a below-average density or mass-to-volume ratio; and (iv) PAS tails are large and disordered.[13] As a result, optical spectroscopy, SDS-based electrophoretic techniques, chromatography, x-ray crystallography, and nuclear magnetic resonance spectroscopy (NMR) are difficult to perform and analyze.[11] With these intrinsic limitations, it can be difficult to raise sufficient analytical evidence supporting the clinical approval of PASylated drugs.

1.5 Acute Lymphoblastic Leukemia (ALL) and Asparaginase

Analogous to the familiar insulin example mentioned at the beginning, this report focuses on a long-acting-asparaginase drug, another established BPD, used to treat acute lymphoblastic leukemia (ALL). ALL is a common childhood cancer that affects 1.1 to 2.1 per 100,000 children

worldwide.[14] ALL results from the rapid abnormal development of certain white blood cells, called lymphoblasts, that eventually crowd-out the healthy white blood cells, causing serious health effects.[15] In 1953, Kidd et. al discovered that guinea pig serum had anti-leukemic properties, and in 1961, J.D. Broome identified that the active anti-leukemic agent in guinea pig serum was asparaginase.[16,17] Asparaginase is an enzyme that converts asparagine (Asn) to aspartic acid (Asp) via a deamidation mechanism. Asparaginases are homo-tetramers that have four active sites that bind Asn cooperatively. In principle, healthy cells produce their own asparagine; however, ALL cells are deficient in the key enzyme: asparagine synthetase.[18] Therefore, ALL cells rely on extracellular Asn to proliferate. By administering asparaginase into the blood serum, serum Asn is consumed causing the cancer cells to starve, while the healthy cells remain undisturbed.[17]

The first clinical use of asparaginase was in 1966; this asparaginase was derived from *E. coli.* Over the past 60 years, advances in biotechnology and recombinant DNA have allowed researchers to modify asparaginase to decrease its immunogenicity, improve manufacturing efficiency, and increase the half-life. To date, the latest approved asparaginase drug is Jazz Pharmaceutical's Rylaze. Rylaze is a recombinant *Erwinia chrysanthemi* asparaginase expressed in a highly efficient *Pseudomonas fluorescens* expression system.[19] Rylaze has low immunogenicity, compared to the *E. coli* derived enzyme, and can be produced in large quantities. Yet, Rylaze has a short serum half-life, furthering the demand for a long-acting asparaginase that will alleviate the frequent dosing, long-hospital stays, and high costs burdened on ALL patients.

1.6 PASylated Asparaginase: JZP-341

Long-acting PASylated recombinant asparaginase: JZP-341, is a current pre-clinical drug candidate produced by Jazz Pharmaceuticals. JZP-341 is a bio-better of Rylaze – the two drugs have the exact same core enzyme and differ only by the addition of the PAS tail on JZP-341. JZP-

341 possesses a PAS tail on each of its four monomers, with a total molecular weight of 204 kDa. Theoretically, the addition of the PAS tail should not affect the biophysics or enzymatic activity of the core asparaginase. However, during the early production of JZP-341, researchers are unable to produce high quality and reproducible batches of the therapeutic. Further, the analysis of JZP-341 is limited by the challenges outlined in section 1.4. Therefore, unique analytical approaches must be taken to characterize the effect of the PAS tail on JZP-341.

1.7 Foundations of Capillary Electrophoresis

We implement different modes of capillary electrophoresis (CE). CE is a powerful analytical technique used to separate molecules in an electric field (E). Molecules migrate with different velocities (v) where $v = \mu E$.[20] μ, the electrophoretic mobility of a molecule, is proportional to a molecule's charge-to-size ratio. Therefore CE separation is based on charge-to-size differences of molecules. The separation is driven by electroosmosis.[21,22] Electroosmotic flow is generated inside the capillary due to the negative charge of the silica wall at pH greater than 3. Cations in the buffer are attracted to the negatively charged wall, creating an adsorbed and diffuse double layer. When voltage is applied, the diffuse layer travels towards the cathode and moves the bulk solution along with it – generating a net flow of solution towards the cathode. A basic CE instrument consists of a high-voltage power supply, a sample injection system, a cooling system, a silica capillary, a detector and an output device.[23] Likewise, at minimum a CE experiment requires an electrolytic running buffer and analyte. Different injection parameters, running buffers, and analytes give rise to different modes of CE such as capillary gel electrophoresis (CGE), capillary isoelectric focusing (cIEF), etc.[22] In this project we use CE in a variety of modes to investigate different properties of JZP-341.

1.8 Foundations of Mass Spectrometry

Like CE, mass spectrometry (MS) is another powerful technique used to separate molecules in an electric and magnetic field. Mass spectrometers can also be used to measure the weight of molecules. A basic MS experiment consists of an ion source, a mass analyzer, and a detector. The most common ion source is an electrospray ionization probe (ESI).[24] ESI involves injecting a liquid sample into a charged thin metal capillary with a narrow tip designed to nebulize the sample into fine charged droplets.[24,25] The charged droplets repel and divide, and the solvent evaporate with the help of dry nitrogen gas until the analyte ions transfer to the gas phase.[26,27] The gas phase ions enter the mass analyzer where they can be filtered with quadrupoles, fragmented in collision cells, or focused by ion optics into a time of flight analyzer. [28] Mass analyzers can be hyphenated to give rise to different modes of MS such as triple quadrupole, or quadrupole time-of-flight.[28] Mass spectrometry can also be used as a detector for liquid chromatography, gas chromatography, and capillary electrophoresis experiments to obtain an in depth understanding of an analyte.

1.9 Research Objective

This project aims at leveraging a variety of instrumental techniques, such as CE and MS, with novel methodologies to better understand the effect of the PAS tail on JZP-341. Herein, we explore three avenues of research in attempts to characterize JZP-341. Chapters 2-4 of this thesis describe our attempts to characterize the structure of JZP-341, to understand the charge heterogeneity of JZP-341, and to identify the enzymatic activity of JZP-341, respectively. We utilize various modes of capillary electrophoresis, mass spectrometry, and chromatography to answer our research goals.

Chapter Two: Structural Analysis of JZP-341

2.1 Protein Structure Analysis by Capillary Electrophoresis

Protein folding and structure is governed by thermodynamics and kinetics. The native-state of a protein is its most-stable or lowest-energy conformation. In literature, PAS tails exhibit a natively disordered structure, with an absence of any secondary or tertiary folding due to the small size and lack of charged functional groups on the Pro, Ala, and Ser residues.[9] However, since protein structure is closely linked to function, it is important to investigate the PAS tail structure on JZP-341 to confirm it is truly inert. We hypothesize that the PAS tail may present in more than one conformation which may result in irreproducible analysis of JZP-341. We aim to determine if thermodynamically stable conformers of the PAS tail exist, and if so, are the conformers kinetically trapped, and do the conformers differ based on their enzyme kinetics?

First, we require a method to identify differences in structure between different JZP-341 samples. As described in chapter 1, many common structural techniques such as x-ray crystallography and NMR are incompatible with PAS tails due to their large and disordered nature. Protein structure can also be studied using mass spectrometry techniques such as hydrogen-deuterium exchange (HDX) or ion mobility spectroscopy (IMS). Our project collaborators performed HDX studies and those results are described elsewhere. Here, we probe protein structure with capillary electrophoresis (CE). As described in chapter 1, CE is a highly efficient microfluidic separation technique that is fast, cost-effective, environmentally friendly, and requires minimal sample volumes. Analytes in the capillary migrate through aqueous buffer (capillary zone electrophoresis, CZE) or through cross-linked gel (capillary gel electrophoresis, CGE). Both techniques offer high resolving power when optimized. CZE is capable of separating analytes that differ based on their charge-to-size ratio. Conversely, CGE is capable of separating analytes based on molecular weight (SDS-CGE) or based on charge-to-size and structure (native-CGE). As

described before, denaturing SDS-based assays are incompatible with PAS tails, and therefore, no useful information can be deduced from SDS-based assays. Here, we attempt CZE and native-CGE to study the native form of the drug candidate. To the best of our knowledge, native-CGE with cross-linked stabilized gel buffer has not been performed on modern CE instruments.

2.2 Materials and Methods:

Chemicals and Materials: All chemicals were purchased from Sigma-Aldrich (Oakville, ON, Canada) unless otherwise stated. Fused-silica capillaries with inner and outer diameters of 75 and 360 μm, respectively, were purchased from Molex Polymicro (Pheonix, AZ, USA). Amicon Ultra 0.5 mL Centrifugal filters Molecular weight cutoff 10 kDa were purchased from Millipore (Burlington, MA, US) Fluorescein Amidite (FAM) labelled MutS aptamer sequence, as selected by Drabovich et al.[29] : 5' -FAM CTT CTG CCC GCC TCC TTC CTG GTA AAG TCA TTA ATA GGT GTG GGG TGC CGG GCA TTT CGG AGA CGA GAT AGG CGG ACA CT –3' was purchased from Integrated DNA Technologies (Coralville, IA, USA).

Instruments: All CE experiments were performed with a P/ACE MDQ apparatus (SCIEX, Concord, ON, Canada), equipped with an LIF or UV detection system. Fluorescence of the FAM aptamer was excited at 488 nm with a blue line solid-state laser and detected at 520 nm. JZP-341 was detected using a UV source lamp and a UV/Vis detector with a 280 nm filter. Uncoated capillaries of 50 cm were used for all CZE and CGE experiments, with inner diameters of 75 μm and 50 μm, respectively. The exterior polyimide coating of the uncoated capillaries was burned using a lighter at 10.2 cm from the outlet.

JZP-341 Preparation: 500 μL of 1 g/L JZP-341 reference standard in formulation buffer and formulation buffer blank was filtered using a 10 kDa MWCO column at 14000 rcf for 10 minutes. The filtrate was discarded and the volume remaining in the column was diluted with 450 μL of 50

mM Tris-HCl pH 7 for buffer exchange. The diluted sample was filtered again at 14000 rcf for 10 minutes, filtrate was discarded, and the remaining protein sample was collected by inverting the filter in a clean vial and centrifuging at 5000 rcf for 5 minutes. The final buffer exchanged concentrated protein sample (10 g/L) was used for all CZE and CGE analysis.

CZE separation: The sample was injected with 0.5 psi for 15 s. Sample Buffer (SB) and Running Buffer (RB) used was 50 mM Tris-HCl pH 7. The sample plug was propagated past the uncooled region of the capillary with RB using 0.9 psi for 30 seconds. The sample was separated at 10 kV for 80 min, unless specified otherwise.

Native-CGE Gel Buffer Preparation: 10 % (w/v) Dextran (450 kDa-650 kDa avg weight), 4% (w/v) Boric Acid, 2 mM EDTA, 10 % (v/v) Glycerol, were combined and the pH adjusted to 8 with Tris Base. The buffer was left to spin gently over 48 hours at room temperature or until dextran had dissolved. Before use in the CE, the buffer was centrifuged at 5445 g for 3 minutes.

Native CGE Separation: Samples were analyzed in a conditioned 50 cm bare silica capillary. See Appendix for conditioning and separation protocols.

2.3 Results and Discussion

We used CE to determine the extent of structural heterogeneity in JZP-341 samples. The presence of structural heterogeneity is indicated by observing multiple peaks or peak broadening in the CZE and CGE electropherograms. CZE can be used to resolve JZP-341 structural conformers. In a CZE experiment with 50 mM Tris-HCl pH 7 running buffer, we detected native JZP-341 directly using UV detection at 280 nm, **Figure 1.** We observed a broad protein peak from 23–37 min. The main peak has a distinct shoulder from 30-37 minutes. The shoulder of the main peak may indicate structural heterogeneities within the protein sample that produce variations in electrophoretic mobility. We attempted to collect this main peak into two 20 μL fractions of 50

mM Tris-HCL pH 7 for repeat CZE-UV experiments, **Figure 2**. We observed an unstable current during fraction collection due to rapid buffer depletion at the outlet end during fraction collection. Further, we re-injected the collected fraction to investigate the conformer stability, however, no peaks were observed due to the significant dilutions during fraction collection and re-injection.

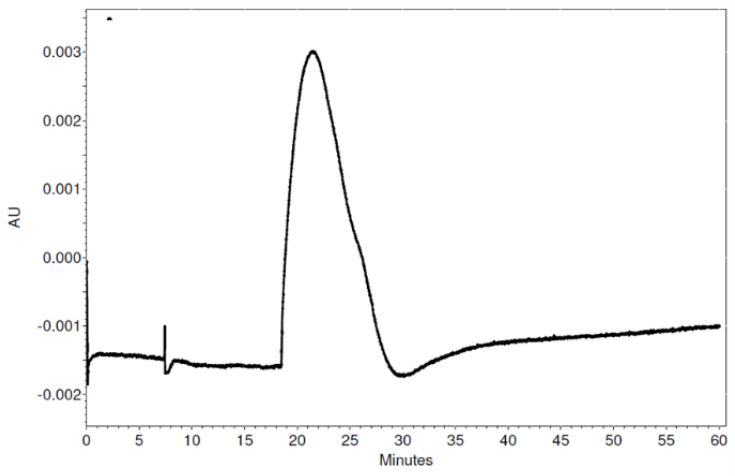

Figure 1 A- CZE-UV 280 separation of 6.6 g/L JZP-341 reference standard in 50 mM Tris-HCl pH 7. 20 kV separation forward polarity.

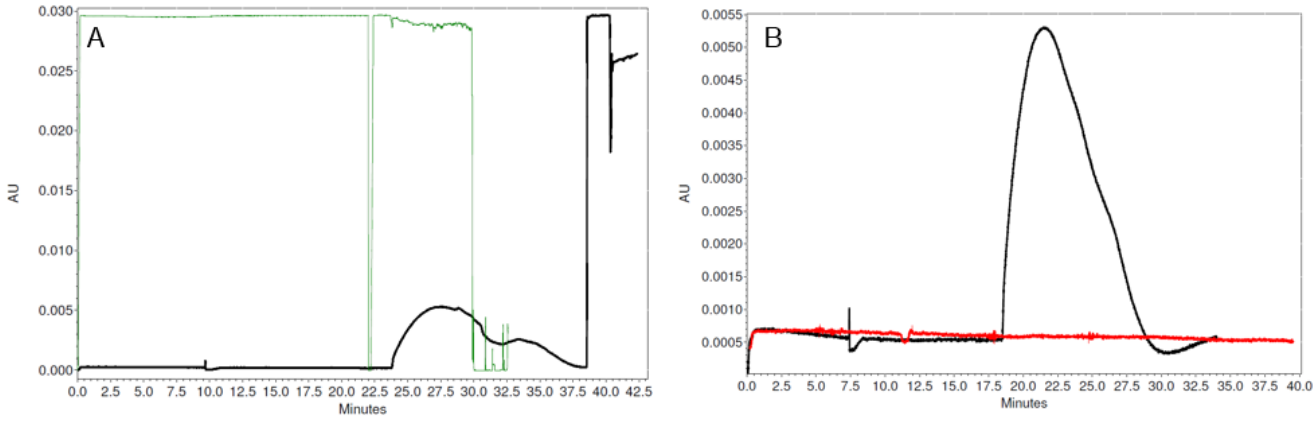

Figure 2 A- Electropherogram of 6.6 g/L JZP-341 reference standard separated at 10 kV (black) Fractions collected from 22-31 minutes, and 31- 32.5 minutes into 20 uL of 50 mM Tris-HCl pH 7. Current profile is overlayed in dark green. B- Electropherogram of fraction 1 (red) compared to original JZP-341 profile (black)

In CGE, analytes migrate through a cross-linked gel through one of many possible unique paths, providing greater separation efficiencies for species with subtle differences in structure. We prepared our native-CGE gel polymer in-house based on an SDS-CGE gel buffer protocol.[30] To

test the separation efficiency of our native CGE gel buffer, we analyzed a fluorescently labelled DNA aptamer. We observed a sharp and narrow peak at 30.8 min with a peak width of 0.2 min, **Figure 3B**. This sharp band suggests high separation efficiency, and minimal longitudinal diffusion of the sample during separation due to the high viscosity of the buffer. However, when we performed native-CGE with UV detection at 280 nm with JZP-341, we did not observe any peaks even after 200 minutes of separation, **Figure 4**. This is likely due to the low sensitivity of UV detection, small injection volume, and slow mobility of JZP-341 in the gel matrix.

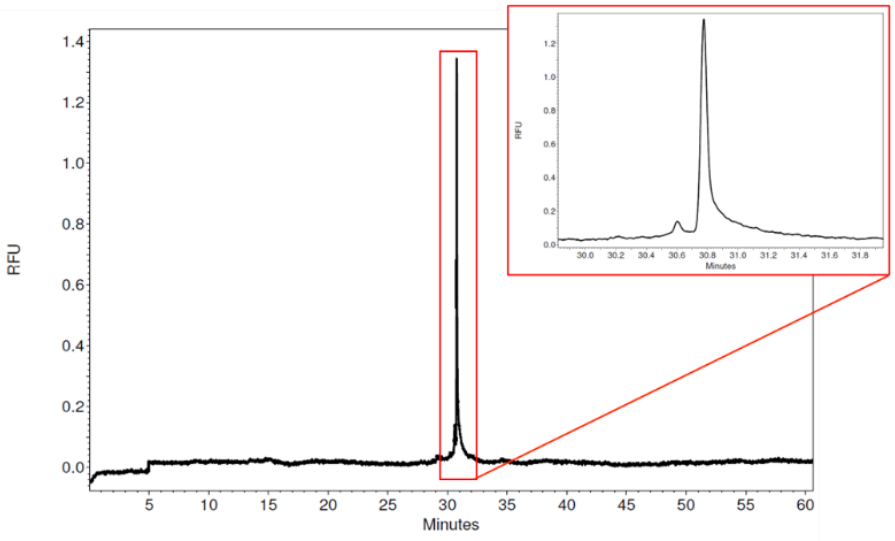

Figure 3-Native- CGE-LIF separation of 333 nM FAM labelled MutS aptamer in 50 mM Tris-HCl pH 7. 30 kV separation reverse polarity

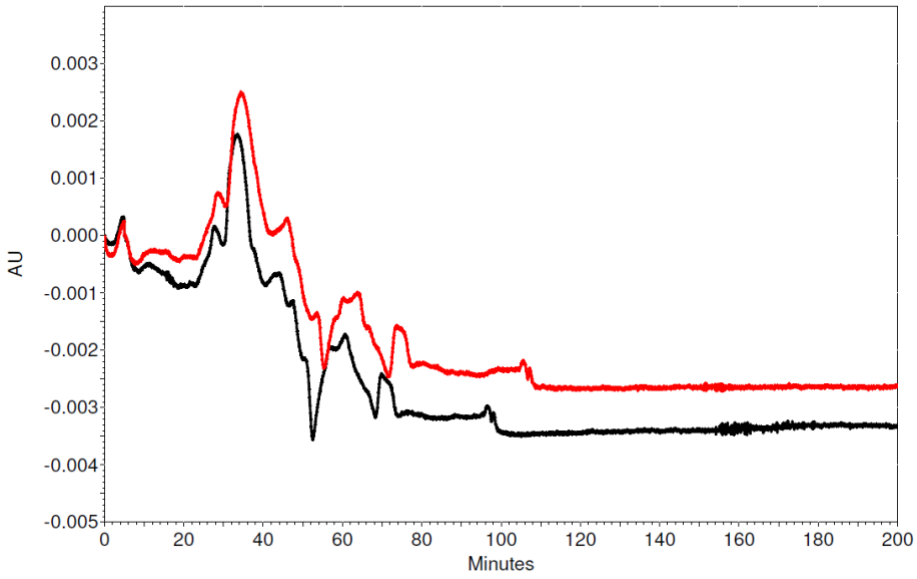

Figure 4 Native-CGE-UV 280 electropherogram of 10 g/L JZP-341 reference standard (black) and 10x Formulation buffer (red)

2.4 Conclusions and Future work

To conclude, CZE analysis of JZP-341 reveals charge-to-size heterogeneity within a sample. These charge-to-size differences are likely a result of structural heterogeneity affecting the mobility of the protein through the capillary. Further analysis is limited by the nanoliter nature of the assay preventing fraction collection and by the low-sensitivity of UV detection. CZE separation coupled to a time-of-flight MS detector with a minimal dilution interface solution can be implemented to achieve higher resolution structural information of JZP-341.

We also present the foundations of a novel native-CGE assay that can successfully detect fluorescently charged DNA aptamer. However, the native-CGE was unsuccessful at separating and detecting JZP-341, likely due to the low sensitivity of UV detection, small injection volume, and slow mobility of JZP-341 in the gel. The native-CGE assay can be used to identify structural conformers of JZP-341 with further optimization of the gel viscosity, injection parameters and detection. A native-CGE assay can also be used to confirm the purity of other BPDs. Further, since

native-CGE does not use surfactants, we can couple native-CGE with a time-of-flight MS with a high dilution interface in order to detect and identify the separated conformers.

Chapter Three: Charge Heterogeneity Analysis of JZP-341

3.1 Charge Heterogeneity Theory

Next, we investigate the presence of charge variants. The central dogma of biological systems dictates that DNA is transcribed to RNA and RNA is translated to proteins. The central dogma seemingly describes a 1:1 ratio of gene to protein. In actuality, over 1 million proteoforms, from a mere 25,000 genes, have been discovered owing to processes such as alternative splicing and post translational modifications (PTM).[31] PTMs can alter enzyme structure, bonding, function, and charge. PTMs on enzyme drugs can affect pharmacokinetics properties and stability, or cause toxic adverse effects. PTMs can differ between batches, host-cells, or expression events, leading to charge heterogeneity within samples or between batches. Charge heterogeneity is an indicator of drug purity and identity, and regulatory agencies expect charge variants to be thoroughly characterized to elucidate the underlying biochemical root cause of their formation.[32] Namely, deamidation, oxidation, and N-terminal pyroglutamate formation PTMs are commonly found in charge variants.[33]

3.2 Capillary Isoelectric Focusing

We assess charge heterogeneity using another variation of capillary electrophoresis technique: capillary isoelectric focusing (cIEF). In cIEF, analytes are introduced to a pH gradient in a capillary and voltage is applied, **Scheme 2**. Proteins migrate to form focused bands at their isoelectric point (pI) or point of zero net charge within the capillary. Then, the focused bands are chemically or hydrodynamically mobilized to the detection window to visualize the charge heterogeneity of the protein sample.[34]

CIEF can be conducted under native or denaturing conditions. Urea is typically used to denature proteins by disrupting hydrogen bonds and promoting unfolding. Denaturing proteins unmasks buried charged groups that would otherwise remain neutralized through hydrogen-bonds

or salt-bridges. Therefore, the same protein can present with a different pI value depending on if it is analyzed under native or denaturing conditions. Interestingly, asparaginases are difficult to denature, and typically require very high concentrations of denaturing agents.[34] However, we begin by completing the preliminary studies under the recommended denaturing conditions, 3.75M Urea, for JZP-341 production analysis using in-process and reference standard JZP-341 samples. Our attempts at increasing the urea concentration resulted in the destruction of the capillary neutral coating, which prevented further experimentation and native-cIEF experiments.

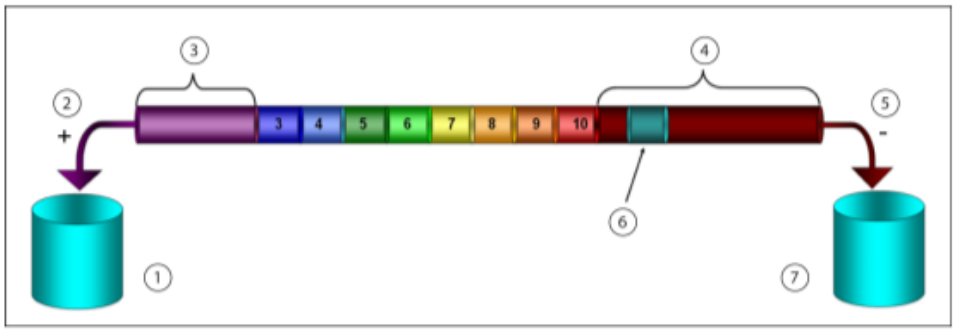

Scheme 2 The pH gradient inside a capillary isoelectric focusing experiment. 1-Anolyte, pH 1.4. 2-Anode. 3- Anodic Stabilizer. 4-Cathodic Stabilizer. 5-Cathode. 6-Detection Window. 7- Catholyte, pH 13.

3.3 Materials and Methods

Chemicals and materials: All chemicals were purchased from Sigma-Aldrich (Oakville, ON, Canada) unless otherwise stated. 3-10 Pharmalyte was purchased from Cytiva. Bare fused-silica capillaries with inner and outer diameters of 75 and 360 μm, respectively, were purchased from Molex Polymicro (Pheonix, AZ, USA). Neutral silica capillaries with inner and outer diameters of 50 and 360 μm, respectively, and cIEF kit (A80976) were acquired from SCIEX (Concord, ON, Canada).

Instruments: All CE experiments were performed with a P/ACE MDQ apparatus (SCIEX, Concord, ON, Canada), equipped with a UV detection system.

cIEF: 500 μL of 1 g/L JZP-341, DSP1 and DSP2 were filtered using a 10 kDa MWCO column at 14000 rcf for 10 minutes. The filtrate was discarded and the volume remaining in the column was diluted with 450 μL of 50 mM Tris-HCl pH 8 for buffer exchange. The diluted sample was filtered again at 14000 rcf for 10 minutes, filtrate was discarded, and the remaining protein sample was collected by inverting the filter in a clean vial and centrifuging at 5000 rcf for 5 minutes. The final buffer exchanged concentrated protein sample (10 g/L) was used for all cIEF analysis. 50 ug of sample up to 10 uL was combined with cIEF Master Mix: 200 μL 3.75 M Urea-cIEF gel, 12 μL pharmalyte pH 3-10 carrier ampholyte, 20 μL cathodic stabilizer (500 mM arginine), 2 μL anodic stabilizer (200 mM iminodiacetic acid), and 2 μL of each pI marker. See **Appendix** for conditioning, separation, and shutdown protocol. The separation was performed on a 30 cm neutral capillary with a detection window 20 cm from the outlet end. UV absorbance was collected at 280 nm. Sample storage was set to 10°C, capillary coolant temperature was set to 20°C.

3.4 Results and Discussion

We performed cIEF analysis of JZP-341 reference standard, in-process column eluant (DSP2), and in-process column strip/discard (DSP1), **Figure 5.** This analysis is performed under denaturing conditions (3.75 M Urea) which exposes buried charged peptides. We quantified the pI of the observed peaks by interpolating from a calibration curve of the protein markers of known pI vs time, **Figure 5A**. JZP-341 reference standard presents with a main peak at a pH of 7.19 and a relatively small acidic and basic shoulder, indicating that the sample has some heterogeneity, **Figure 5B**. The reference standard profile is our positive control.

Throughout the protein production, process samples are purified. Here, we see the results of column purification. The column eluant has one main peak at pH 7.3 and a sharp acidic shoulder at 7.13, **Figure 5C**. The column strip has multiple basic peaks and a main peak at 7.67, **Figure**

5D. Based on qualitative comparison, the column eluant is more similar to the reference standard than the column strip, suggesting that the column purification was effective at removing most of the basic charge variants, leaving behind the desired product with a pI of 7.2-7.3.

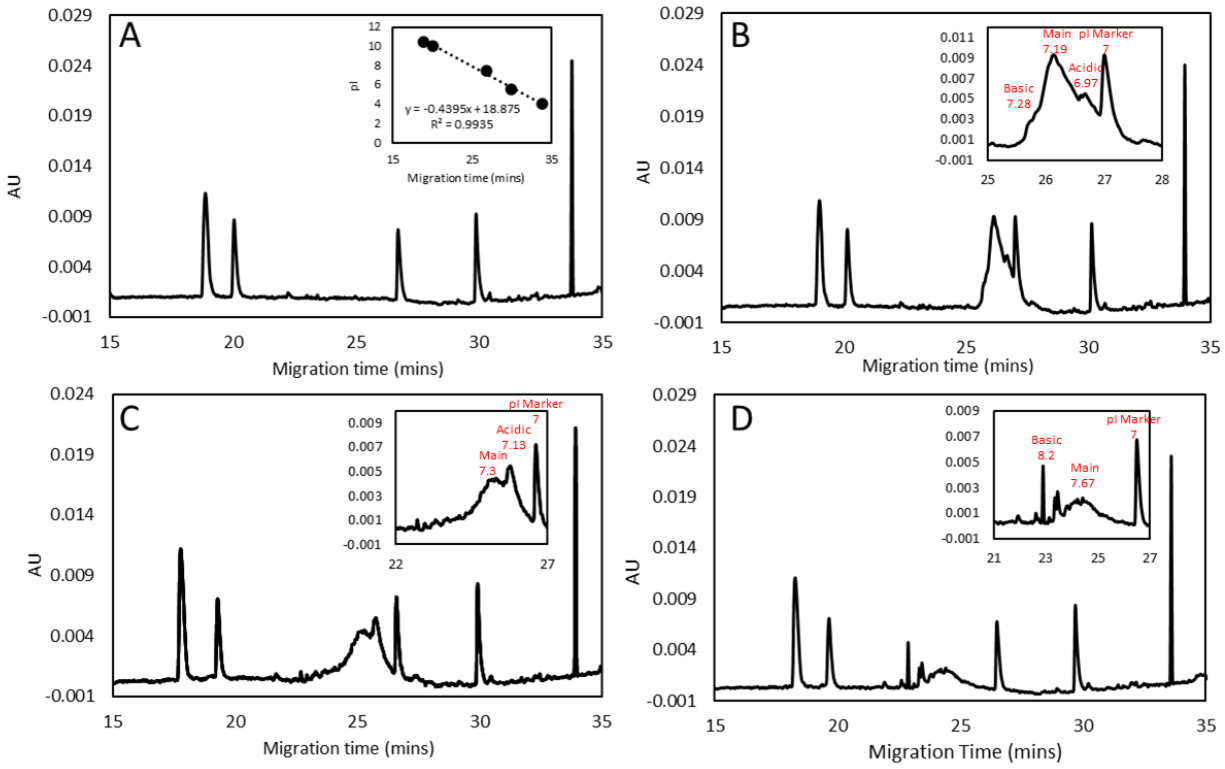

Figure 5 cIEF of JZP-341 reference standard and in-process samples, detection=280 nm. A- Negative control pI markers 4, 5.5, 7, 10, 10.5, from right to left. Calibration curve inset y=-0.4395x+18.875 R2=0.9935. B- JZP-341 reference standard drug substance. C-DSP2-Gigacap column eluant. D-DSP1-Gigacap column strip. Insets of B-C show zoom in of sample profile.

3.5 Conclusion and Future Work

We used a commercial cIEF kit to deduce differences between different production samples of JZP-341. We observe minimal heterogeneity for the reference standard and column eluant samples, while the column strip contained basic variants. Our analysis confirms that in-process column purification of JZP-341 was successful. Negative controls with a known pure protein should be performed to validate the protocol. Native cIEF analysis should be performed to determine the effect of 3.75 M urea on JZP-341, and high concentrations of urea should be avoided

to maintain the integrity of the capillary coating. Overall, cIEF was a fast and simple methodology to implement for determination of JZP-341 charge heterogeneity.

Chapter Four: Kinetic Analysis of JZP-341

4.1 Enzyme Drugs

Enzymes, like JZP-341, catalyze essential reactions involved in metabolism, immune response, and reproduction of living systems.[35] Moreover, enzymes can be synthesized and used in a variety of industries such as food, fuel, and therapeutics.[36] Enzyme replacement therapies have shown efficacy in the treatment of human diseases that result in inactive, dysfunctional, or absent enzymes.[35] Additionally, enzymes can be implemented strategically in the treatment of cancers, infections, and wounds.[35] Like any other drug, enzyme therapies must be rigorously tested for critical quality attributes such as identity, quantity, potency, efficacy, and purity.[37] However, contrary to its small molecule drug counterparts, enzyme analysis is tedious as structure, charge, and enzyme activity must be maintained throughout the manufacturing process.

4.2 Enzyme activity

Enzyme activity is an indicator of drug efficacy and potency. Therefore, it is important to have an enzyme activity assay for the assessment of JZP-341. Enzyme activity is commonly studied under the steady-state approximation. We consider a bimolecular reaction between enzyme (E) and substrate (S) leading to the reversible formation of the enzyme substrate (ES) complex. Next, the ES complex can irreversibly react to form the product (P) and the free enzyme (E):

$$E + S \rightleftharpoons ES \rightarrow E + P$$

Where $[E]_{total} = [E]+[ES]$. At high [S], we assume that all $[E]_{total} = [ES]$, $d[ES]/dt = 0$, and the reaction speed is proceeding at maximum velocity (V_{max}) – this is the steady-state. With mathematical transformations we can deduce the Michaelis Menten equation:

$$V_o = \frac{V_{max}[S]}{K_m + [S]}$$

Where V_o is the initial reaction rate (velocity) and K_m is equal to [S] where $V_o = \frac{V_{max}}{2}$. A Michaelis-Menten plot will show the hyperbolic relationship between [S] and V_o.

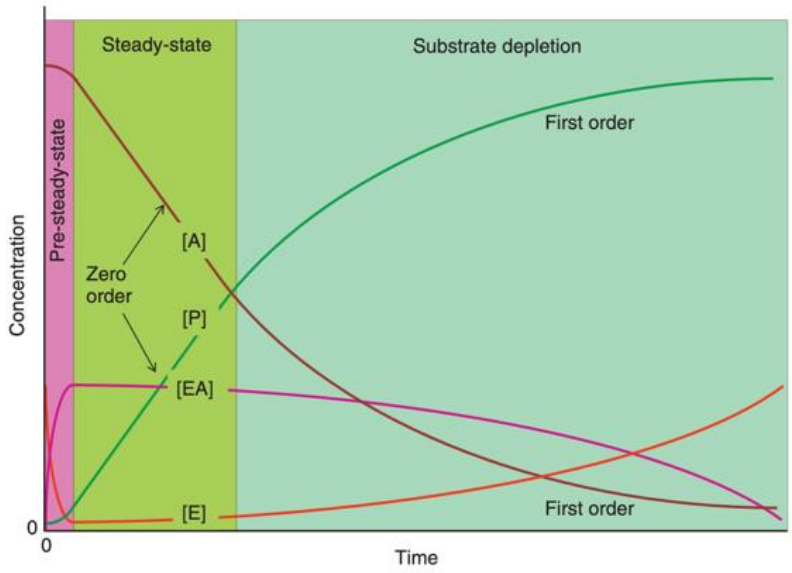

Scheme 3 Plot of concentration of substrate (A), product (P), enzyme substrate complex (EA) and free enzyme (E) over time. The three phases of a reaction are the pre-steady state, the steady-state, and the substrate-depletion state. Adapted from ref [38]

A plot of substrate and product concentration vs. time demonstrates different reaction-order regimes at different phases in the reaction, **Scheme 3**. At the steady state, we observe a linear relationship (zero-order kinetics) with a slope of V_o, until the [S] approaches K_m.[38] Hereupon, we define an activity assay as the measurement of V_o during the steady-state. Experimentally, activity assays should test initial [S] ranging from $0.1K_m$ – $10K_m$, in replicate, to improve accuracy of the Michaelis-Menten plot.[39] When initial [S] approaches K_m, the time spent in the linear portion of the reaction will decrease significantly, making analysis difficult. To circumvent this difficulty, we must (1) ensure the [E] is significantly low which will decrease V_o and increase the linear portion of the reaction, and (2) ensure that the detection method is sensitive enough to observe the turnover at such low concentrations. Unpublished reports of JZP-341 activity suggest a K_m of ~20

μM. Therefore Asn concentrations from 2-200 μM is a suitable range to determine K_m of JZP-341.[40]

In addition to high sensitivity, activity assays must also be highly reproducible and fast, with limited hands-on steps to increase the accuracy of the measurements. Traditional activity assays rely on colorimetric reactions in microtiter plates that require numerous hands-on steps causing significant error, resulting in inaccurate K_m values.[41] Instead, we sought a method that was automated and label-free to obtain fast, reproducible, and accurate results. Lastly, the ideal method will be highly sensitive and not susceptible to matrix effects so that the whole range of enzyme drug production samples can be analyzed.

4.3 Types of activity assays

Enzyme activity assays are highly specific to the catalysis reaction resulting in a variety of enzyme-specific methods. Current attempts at confirming and maintaining enzyme functional activity include plate-based and separation-based techniques using optical or mass detection. These methods are limited by sensitivity, matrix interference, and lack of automation.[41] Plate-based methods usually involve coupled-reactions or non-native chromogenic substrates that can be detected using a plate-reader and quantitated against a calibration curve. Plate-based methods require highly pure samples, involve numerous pipetting steps, and have low sensitivity. These methods are not compatible with enzyme samples from early production steps with complex matrices. Chromatographic techniques involve manual preparation of the enzyme reaction, on-capillary or off-capillary labelling, followed by chromatographic separation and optical detection.[42] Mass spectrometric methods are also limited by manual preparation of the enzyme reaction, and low resolution of some substrate and product pairs.[42]

4.4 Inject-Mix-React-Separate-Quantitate Capillary Electrophoresis Activity Assay

CE can also determine enzyme activity. An established CE-based activity assay developed by the Krylov group called Inject, Mix, React, Separate and Quantitate (IMReSQ).[43] IMReSQ begins with short consecutive injections of enzyme (E), substrate (S), and enzyme buffer (EB) as separate plugs into a capillary prefilled with running buffer (RB). The plugs are mixed inside the capillary by transverse diffusion of laminar flow profiles and catalysis begins. After a prescribed reaction time, the enzyme reaction is terminated by applying voltage across the capillary and then the substrate and product are separated and quantitated, **Scheme 4**. By changing the incubation time, we can monitor the speed of catalysis, and by testing different initial [S] we can extrapolate K_m. IMReSQ is completely automated, speedy, and requires only nanoliter volumes of reactants. Another major advantage of IMReSQ is its compatibility with EB and RB mismatch. To elaborate, most enzymes require physiological conditions (pH, salt) to function at their maximum activity. However, physiological buffers often result in very high current in CE which can be detrimental. In an IMReSQ experiment the enzyme reaction can proceed at the capillary inlet in a physiological EB, while the remainder of the capillary is filled with a CE-compatible RB.

Furthermore, IMReSQ has been coupled with different optical and mass detectors for substrate discovery, inhibitor discovery, cofactor analysis and enzyme activity applications.[43–45] We investigate native and fluorescently labelled Asn and Asp with UV and LIF detection, respectively, for IMReSQ analysis. Parameters such as RB, injection order, choice of internal standard, buffer mismatch, and substrate concentration for analysis of JZP-341 are optimized, some of these efforts are described here. However, due to inefficiencies of fluorescent labelling and low sensitivity of UV absorbance restricting us to mM initial substrate concentrations, we shift to mass spectrometry (MS) detection.

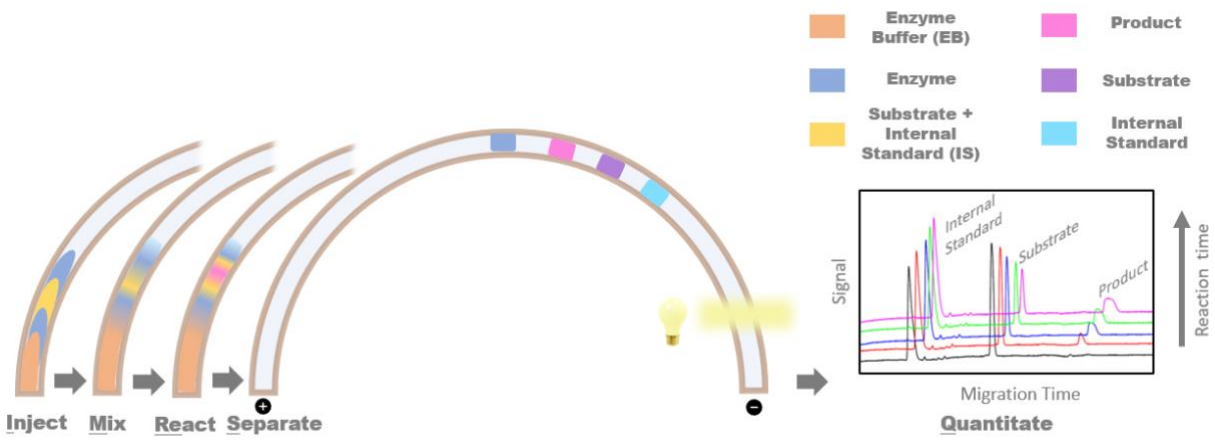

Scheme 4 : 5 steps of IMReSQ 1. Inject: nanoliters of enzyme, substrate + internal standard, and enzyme buffer are injected in the order shown above. 2. Mix: reagents to mix by transverse diffusion. 3. React: enzyme begins on-capillary catalysis for a prescribed amount of time. 4. Separate: the reaction is stopped by applying voltage and separating the substrate, product, internal standard, and enzyme based on electrophoretic mobility 5. Quantitate: Peak areas are used for quantitation.

4.5 Capillary Electrophoresis-Mass Spectrometry IMReSQ

CE-MS is a powerful hyphenated technique as it combines high-efficiency separation with mass detection and identification.[46] However, since both CE and MS are electrically driven fluidic techniques with different voltage, flow rate and buffer requirements, much attention must be given to the interface.[47] For example, CE separations work best with aqueous electrolytic buffers while MS requires volatile buffers with no salt to avoid ion suppression. IMReSQ-MS has been previously reported for other enzymes using a sheath-flow interface (SFI).[44,45] SFI is a co-axial strategy where the sheath fluid (SF) is contained around the capillary and allowed to mix with the capillary flow right before nebulization, **Scheme 5**. In general, co-axial SFIs provide minimal dilution which restricts the CE experiment to volatile RBs.[48] However, similar to what was described earlier, it is not ideal to perform IMReSQ-MS with volatile RB or EB as it hinders the catalytic activity of certain enzymes and can affect separation efficiency.

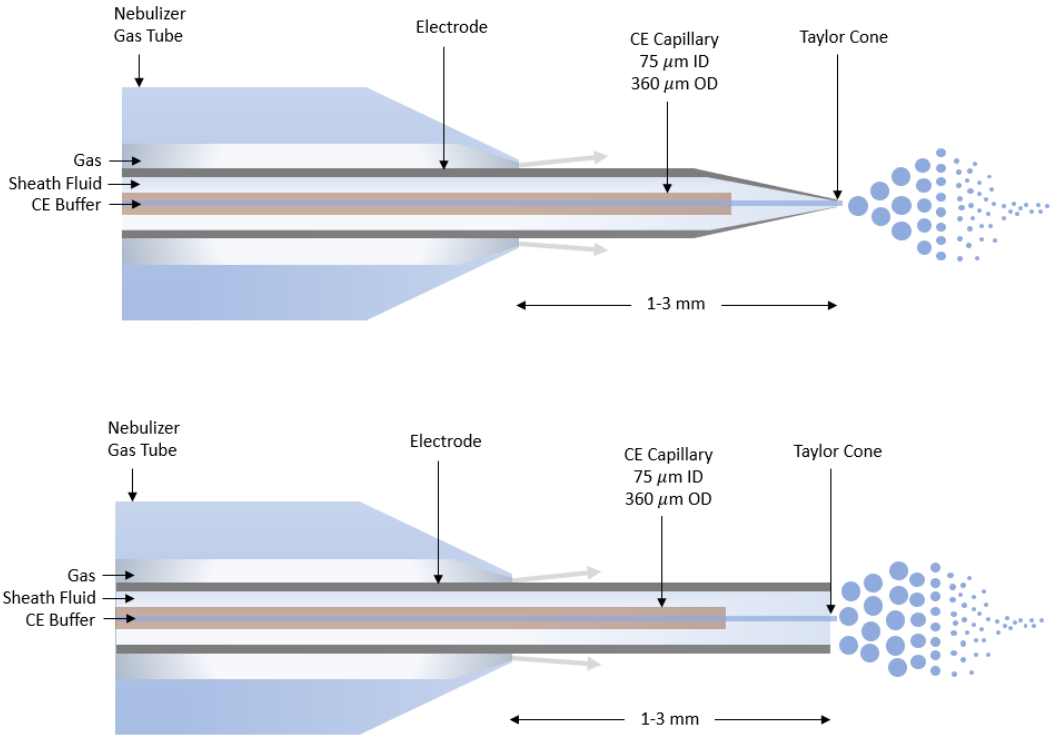

Scheme 5 Common sheath-flow CE-MS interface for electrospray ionization. Top tapered electrode, bottom non-tapered electrode.

To overcome the limitations of the SFI, we turn towards a novel open-port interface (OPI). OPI was first reported in 2015 and has since been adapted to use in different liquid-MS applications.[49] OPI separates the electrical circuit of the CE from the MS and significantly dilutes the capillary flow 100-times with a volatile SF, **Scheme 6**.

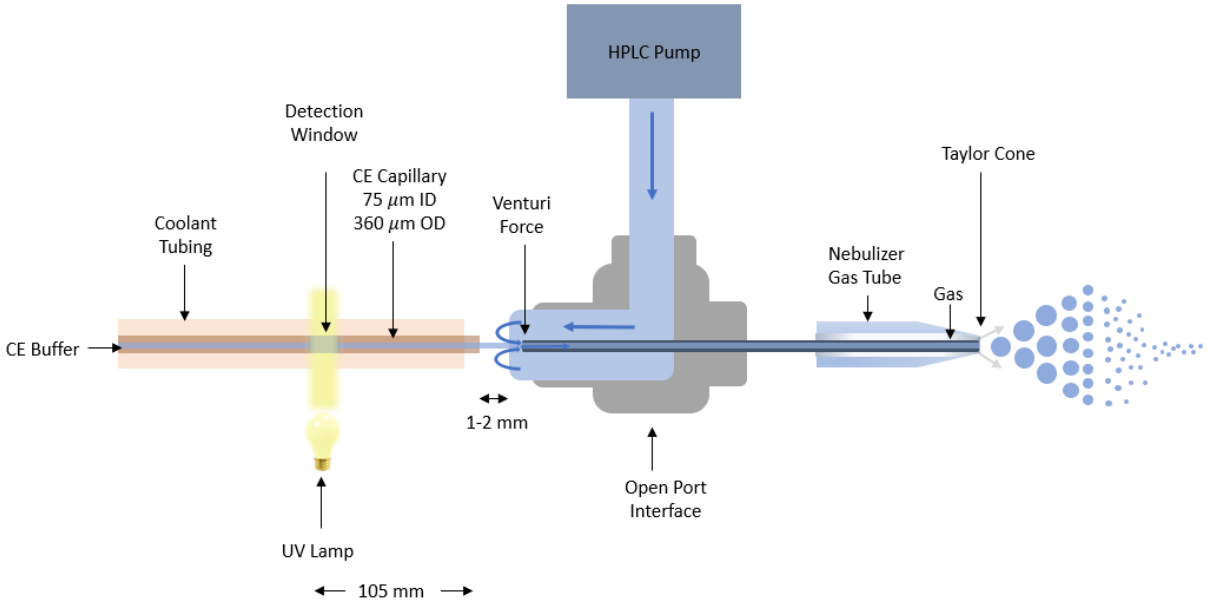

Scheme 6: Open-port CE-MS Interface. Capillary outlet is placed a few millimeters away from the interface where it meets the sheath-liquid vortex. The sheath-liquid vortex is supplied by an HPLC pump. Capillary flow is drawn into the vortex by venturi force (assuming constant mechanical energy, venturi force describes the increase in fluid velocity as it passes through a constricted area.

Therefore, OPI can liberate CE-MS from the use of volatile buffers, making the OPI beneficial for IMReSQ experiments that involve physiological EB and CE-friendly RB.

4.6 Materials and Methods

Chemicals and Materials: All chemicals were purchased from Sigma-Aldrich (Oakville, ON, Canada) unless otherwise stated. Fused-silica capillaries with inner and outer diameters of 75 and 360 μm, respectively, were purchased from Molex Polymicro (Pheonix, AZ, USA). Chromeo P503 pyrylium dye was purchased from ActiveMotif (Burlington, ON, Canada). Alexa Fluor 488 5-TFP was purchased from Invitrogen (Waltham, MA, US). Amicon Ultra 0.5 mL Centrifugal filters Molecular weight cutoff 10 kDa were purchased from Millipore (Burlington, MA, US)

Instruments: All CE experiments were performed with a P/ACE MDQ apparatus (SCIEX, Concord, ON, Canada), equipped with an LIF or UV detection system. Fluorescence of the

ALEXA labelled amino acids was excited at 488 nm with a blue line solid-state laser and detected at 520 nm. Fluorescence of the Chromeo-labelled amino acids were excited at the same length and detected at 630 nm. Native Asn and Asp were detected using a UV source lamp and a UV/Vis detector with a 200 nm filter. Uncoated capillaries of 50 cm were used for experiments. The exterior polyimide coating of the uncoated capillaries was burned using a lighter at 10.2 cm from the outlet. All stand-alone MS experiments were performed with an API 5000 apparatus equipped with a Turbo V Ion Source and ESI probe (SCIEX, Concord, ON, Canada). CE-MS experiments at SCIEX were performed on a TripleTOF 6600+.All HPLC experiments were performed on an Agilent InifinityLab LC/MSD 1260 system equipped with a 1260 Infinity II Diode Array Detector HS (Santa Clara, CA, US).

ALEXA-488 Labelling: 10 mg of Asn and 10 mg of Asp were each dissolved in 1 mL 0.1 M sodium bicarbonate buffer to prepare a 75 μM solution. 3 μL of 2 mM ALEXA-488 was combined in 497 μL DMSO to prepare an 11 μM solution. 100 μL of 11 μM ALEXA was combined with each of the 1 mL 75 μM amino acid solutions and the samples were vortexed in the dark for 1 hour at RT.

Chromeo Labelling: Chromeo P503 stock solution (1 mg/ 100 μL Dimethylformamide) was diluted 25x in 0.1M $NaHCO_3$ pH 8.3 to obtain a 1 mM working solution 18 μL of 20 mM amino acid solutions were combined with 2 μL 1 mM Chromeo p503. The labelled amino acids were incubated overnight at 4°C.

O-Phthalaldehyde (OPA)/ β-Mercaptoethanol (BME) Labelling: 13 mg OPA was dissolved in 1.3 mL methanol, 2 mL 25 mM sodium tetraborate and 16 µL BME. 500 uL of OPA

solution was combined with 500 uL of 18 mM Asp or Asn in 0.1 M HCl, vortexed, and analyzed within 15 minutes.

RPLC: 50 μL of OPA/BME amino acid solution was injected using an autosampler and separated on an Agilent AdvanceBio Peptide mapping column 2.1x150 mm, 2.7 µm. Eluant A= 100 mM $NaCH_2COO$, Mobile Phase B= 45:45:10 ACN: MeOH: H2O. Column temperature is set to 40°C and flowrate was set to 0.25 mL/min. Gradient program: Time = 0, %B =2; T = 13.4, %B = 57 ; T = 13.5, B = 100; T = 15.8, %B = 2% ; T = 18 = end.

Mass Spectrometry: Samples were introduced using a syringe pump at a flow rate of 5 µL/min. The MS multiple reaction monitoring (MRM) conditions in positive ion mode were as follows: CAD = 5, CUR = 20, GS1 = 20, GS2 = 5, IS = 5500, TEM = 200, DP = 30, EP=10, CE=20, CXP=15. Asn fragments: 133.4 → 46, 133.4 → 74, and 133.4 → 88. Asp fragments: 134.4 → 70, 134.4 → 74, 134.4 → 88, 134.4 → 116.

IMReSQ-UV Separation: Asn, Asp, and internal standards (Lys and Gly) were detected using a UV source lamp and a UV/Vis detector with a 200 nm filter. Samples were analyzed in a conditioned 50 cm bare silica capillary using the following protocol: 20 psi 2 min rinse with 0.1 M HCl, 20 psi 2 min rinse with 0.1M NaOH, 20 psi 2 min rinse with running buffer (RB), and 20 kV 20 minutes separation with RB. Sample storage was set to 4°C, capillary coolant temperature was set to 37°C. See **Appendix** for separation protocols. The capillary running buffer was 25 mM Sodium-borate pH 9.2 (borax) for all experiments. The EB was either borax or phosphate buffered silane pH 7 (PBS). JZP-341 was diluted 10,000x with EB to a final concentration of 0.0001 mg/mL. Asparagine was tested at 6.25 mM and 1 mM and the internal standard was analyzed at 25 mM. Electropherograms were analyzed with 32 Karat Software migration times are corrected

for changes in electroosmotic flow by a 2-point correction method described by the Dovichi lab, Appendix.[50]

IMReSQ-MS Separation: Samples were analyzed in a conditioned 49 cm bfs capillary, 50 um i.d. 10.5 cm UV window. Detection = 214 nm. Sample storage was set to 4C, and no temperature control was used for the capillary. The capillary was rinsed with 1% TFA and 5% NH4OH, and borax buffer, respectively. sequential hydrodynamic injections proceeded in the following order: 0.1 psi for 11 sec enzyme, 0.1 psi for 11 sec substrate and internal standard, 0.1 psi for 11 sec enzyme, and 0.1 psi for 33 sec buffer. After each injection the capillary and electrode were dipped into a vial of water to prevent carry-over to the next vial. Incubation times of 0, 5, 10, 15, and 20 minutes were investigated. Separation was driven by an electric field of 500 V/cm with positive polarity at the capillary inlet. TOF 6600+ conditions in positive ion mode were as follows: SF= 50 H2O, 50 MeOH, 1% Acetic Acid. 100 uL/min GS1=60, GS2=2-, CUR=20, TEM=400, ISVF=5000, CP=1000, DP=80, ITC=0, CE=10, Q0L:34

4.7 Results and Discussion

4.7.1 Investigating fluorescent labelling of substrate and product

CE-MS systems are not always available, therefore we first attempted to develop a CE or HPLC based activity assay with fluorescence detection. Our goal was to find a fast and robust fluorescent labelling method that can be used to develop a high sensitivity IMReSQ experiment. We labelled the amino acids with 3 different dyes: chromeo P503, alexa-488, and O-phthaldehyde/β-mercaptoethanol (OPA-BME).

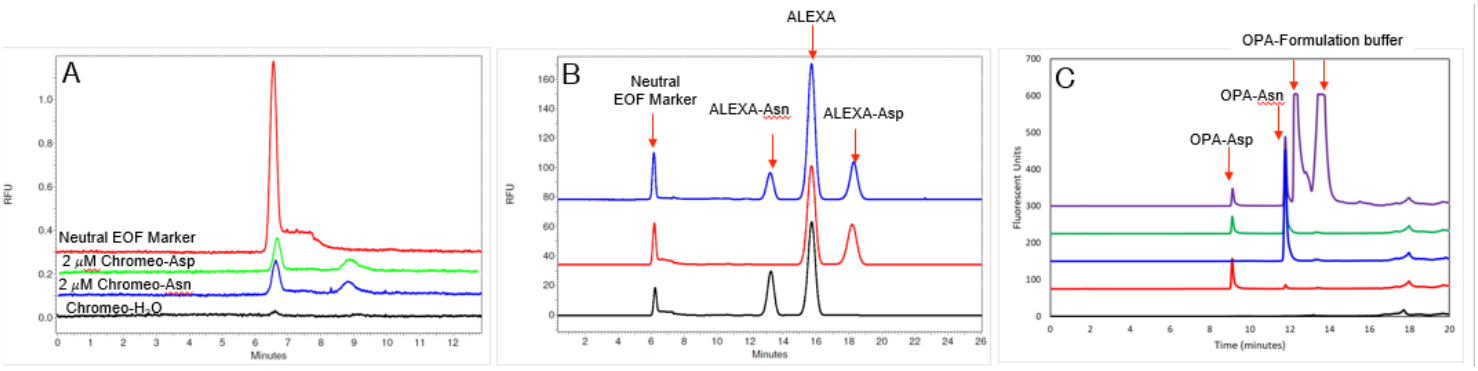

Figure 6 A- CZE separation of 0.1 μM Chromeo-H_2O (black), 2 μM Chromeo-Asn (blue), 2 μM Chromeo-Asp (green), and 125 nM neutral EOF marker bodipy (red). Separation was performed in 25 mM sodium tetraborate pH 9.2 at 5 kV normal polarity. B- CZE separation of 200 nM neutral EOF marker with 2 μM ALEXA-Asn (black), 2 μM ALEXA-Asp (red), and 2 μM ALEXA-Asn and 2 μM ALEXA-Asp (blue). Separation was performed in 25 mM sodium tetraborate pH 9.2 at 10 kV normal polarity. C- RP-HPLC separation of OPA/BME working solution (black), 9 mM OPA-Asp (red), 9 mM OPA-Asn (blue), 4.5 mM OPA-Asn and 4.5 mM OPA-Asp (green), and 3.6 mM OPA-Asn and 3.6 mM OPA-Asp with formulation buffer containing other amino acids (purple).

Chromeo-p503 is a fluorogenic and neutral dye that reacts with primary amines and requires overnight incubation. We analyzed chromeo-Asn, chromeo-Asp with CZE in a 25 mM sodium tetraborate pH 9.2 (borax) buffer, **Figure 6A**. We also analyzed chromeo incubated with water as a negative control to confirm that the dye is fluorogenic, and bodipy, a neutral marker, to determine the migration time of neutrally charged analytes under these conditions. Each amino acid presented with two peaks, the first peak at 6.5 minutes corresponded to a neutral entity, and a second peak at 8.8 minutes corresponded to a negatively charged entity. These peaks overlapped and therefore this labelling method could not be used to resolve Asn and Asp. It is unusual to observe two peaks as there should only be one fluorescent product from a chromeo labelling reaction, and unlabelled chromeo is not fluorogenic, as demonstrated in the negative control: chromeo-H_2O (black trace). One hypothesis for this observation is the formation of dimers. The CZE results, along with the long incubation time rendered chromeo unsuitable to label Asn and Asp.

Next, we attempted to label Asn and Asp with alexa-488 (alexa). Alexa is a large molecule that binds primary amine groups of proteins within 2 hours Alexa is also not fluorogenic, so once labelled, the mixture of alexa-Asn, alexa-Asp, and free alexa must be separated from one another.

Again, we used CZE in 25 mM sodium tetraborate pH 9.2 to observe the labelled amino acids, **Figure 6B**. Unreacted alexa elutes at 15.5 minutes while alexa-Asn and alexa-Asp elute at 13 and 18 minutes, respectively. We obtained complete resolution of the three species with high signal-to-noise ratio, and separated a mixture of the two amino acids (blue trace). This demonstrates that alexa-488 is a good option for future detection and quantitation of Asn and Asp. However, since JZP-341 is formulated in a complex buffer with other amino acids, we hypothesized that matrix peaks or other primary amines in the matrix may interfere with future analysis.

Lastly, we used a highly reactive label: O-phthalaldehyde (OPA) and β-mercaptoethanol (BME). OPA and BME react to form a fluorescent indole with amino acids, within minutes. The fluorescent products are excited at 350 nm and emit at 450 nm, both of which are not compatible with our current CE setups. Instead, we use an HPLC equipped with a lamp and diode array detector to separate and detect OPA/BME labelled Asn and Asp, **Figure 6C**. We obtained resolution of Asn and Asp at 9 and 12 minutes, respectively. We also analyzed Asn and Asp with JZP-341 formulation buffer and we observed additional peaks that approach the Asp peak. It is likely that the resolution of the Asn peak will be affected at high concentrations of protein in its native buffer.

4.7.2 Investigating MS detection of substrate and product

Labelling amino acids introduces long sample preparation time, experimental complexity, potential error, and potential signal overlap. Ultimately, a label-free method is required for fast, accurate, and sensitive enzyme activity determination. Therefore, we analyzed Asn and Asp directly with mass spectrometry (MS). Using multiple reaction monitoring, we can monitor multiple fragments of Asn (132 amu) and Asp (133 amu). We demonstrated high method linearity across 4 orders of magnitude for Asn and 5 orders of magnitude for Asp, **Figure 7A-B**. We cannot

accurately analyze a mixture of Asn and Asp directly because Asn and Asp form the isobaric fragments, and the 1% ^{13}C contribution of Asn (133 amu) overlaps with the main Asp signal (133 amu).[51] Therefore, it is imperative to obtain high resolution between Asn and Asp in IMReSQ prior to MS/MS experiments.

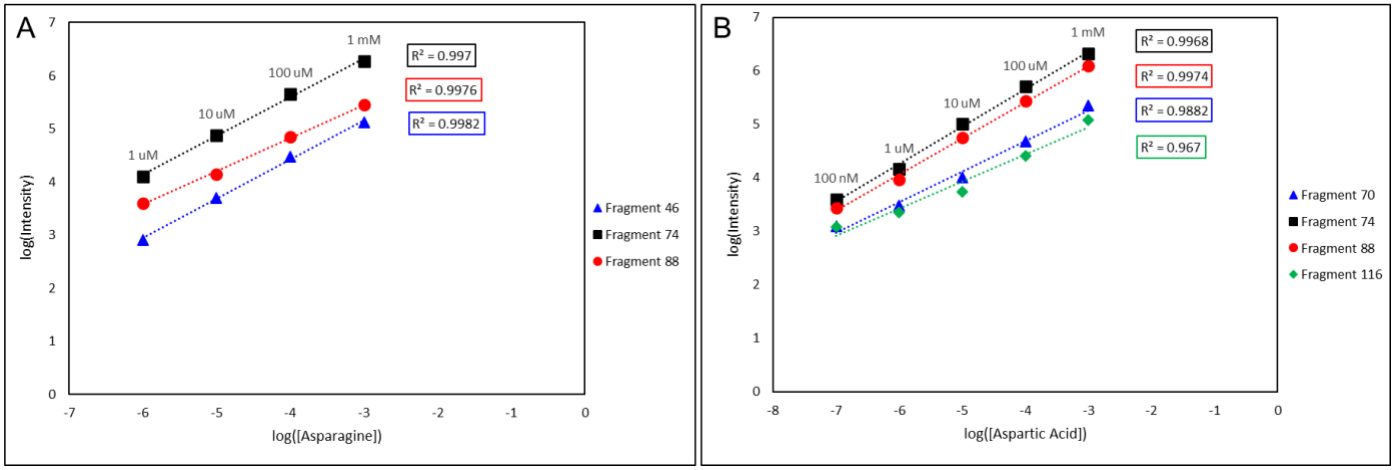

Figure 7 Double log standard curve of Asparagine (A) and Aspartic Acid (B) MRM fragments

4.7.3 Investigating IMReSQ-UV

We monitored the reaction rate of JZP-341 with its native substrate, Asn, via IMReSQ. To do so, we had to find (1) a suitable RB that results in sharp resolved peaks and (2) an internal standard to normalize for differences in injection volume and to quantitate the substrate. We found that borax buffer with UV detection at 200 nm provides excellent resolution and sharp peaks, **Figure 8.** We also determined that lysine (Lys) is a suitable internal standard as it has a similar size and chemical structure to the analyte, Asn, and is well resolved from the Asn peaks.

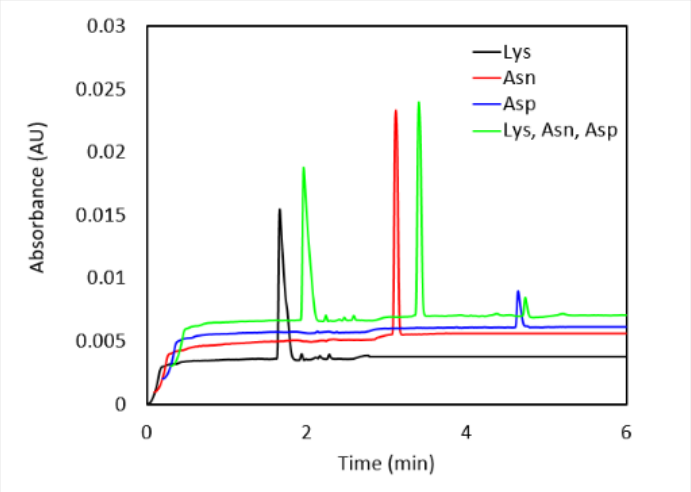

Figure 8 IMReSQ Negative controls. Buffer = 25 mM Sodium tetraborate pH 9.2. 25 mM Lys (Black), 6.25 mM Asn (Red), 1 mM Asp (Blue), 25 mM Lys, 6.25 mM Asn, 1 mM Asp (Green). UV 200 nm detection.

We monitored the reaction over time by performing a series of experiments from 0-, 5-, 10-, 15-, and 20-minute reaction times and observed the consumption of Asn and the production of Asp. However, due to the higher extinction coefficient of Asn, and thus better sensitivity, we only quantified the change in Asn peak area. We used a corrected migration time to correct for changes in the surface chemistry and injection volumes, **Appendix**.

We compared two different initial [Asn]: 6.25 mM and 1 mM, **Figure 9A-B**. In both experiments, RB and EB are borax. We plotted concentration vs. time and fit the data to a linear regression, as we are assuming steady-state kinetics, **Figure 9D**. We observed a decrease in the reaction rate with a lower initial substrate concentration. These findings are in line with Michaelis-Menten enzyme kinetic theory.

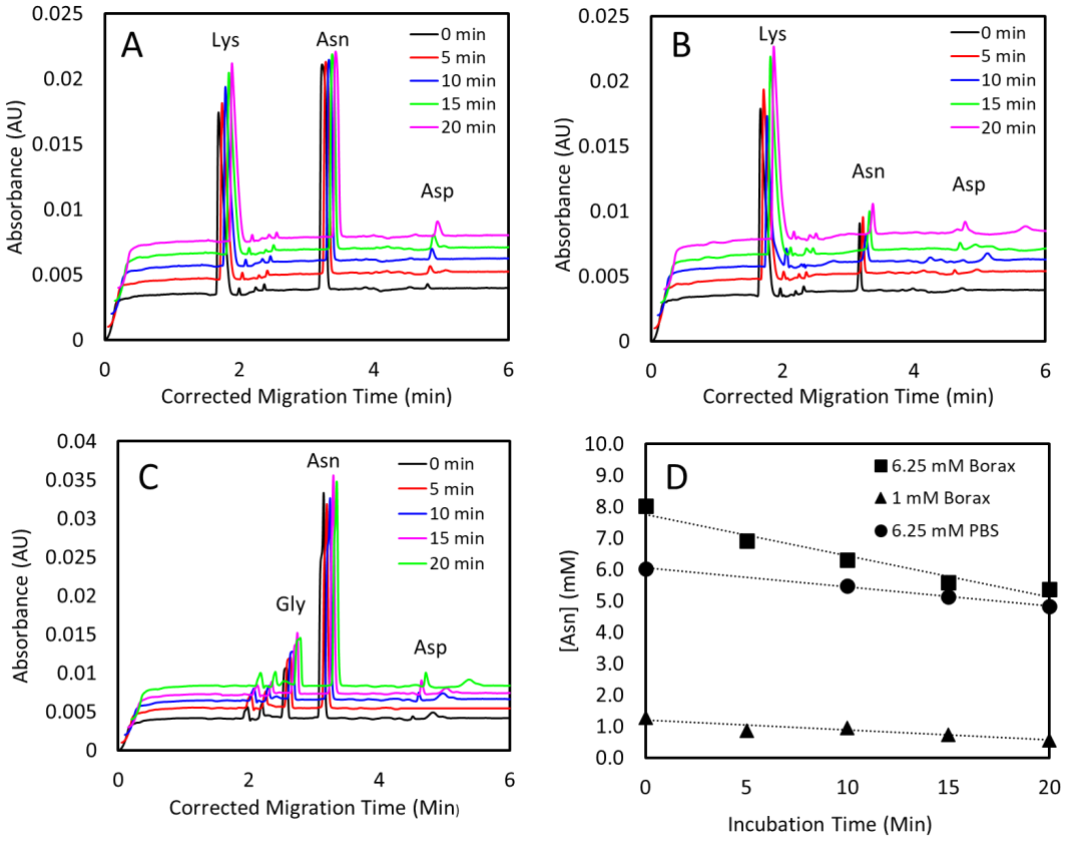

Figure 9: IMReSQ electropherograms of ASNase reaction at 0, 5, 10, 15, 20 minutes reaction times. (A) 6.25 mM Asn, 25 mM Lys IS, 0.0001 mg/mL ASNase in EB and RB= Borax pH 9.3. (B) 1 mM Asn 25 mM Lys IS, 0.0001 mg/mL ASNase in EB and RB= Borax pH 9.3. (C) 6.25 mM Asn 25 mM Gly IS, 0.0001 mg/mL ASNase in EB=PBS pH 7.4 and RB= Borax pH 9.3. (D) Quantitative assessment of [Asn] at different incubation times. [Asn] was determined via internal calibration. Linear regressions and R^2 values: ■ - (A) y=-0.1321x + 7.7576 R^2=0.95159, ● - (B) y = -0.0606x + 6.0505, R^2 = 0.8647 ◢ - (C) y = -0.0312x + 1.1928, R^2 = 0.9974

Next, we performed IMReSQ with a buffer mismatch between the RB and EB, and compare the differences in enzyme reaction. We performed an experiment where the enzyme reaction buffer is PBS pH 7 and the running buffer is borax buffer, **Figure 9C**. At pH 7, Lys is an unsuitable internal standard as it co-migrated with Asn. Instead, we found that glycine (Gly) is a well resolved alternative internal standard. Furthermore, PBS pH 7 is closer to physiological conditions than borax buffer. In general, we expect V_o will be higher in PBS pH 7. However, we observed a slower reaction rate in PBS, **Figure 9D**. Overall, the sensitivity of UV is insufficient for enzyme activity analysis, therefore we used these experimental conditions as the foundation for IMReSQ-MS experiments.

4.7.4 Investigating IMReSQ-MS

We attempted to use the tapered sheath-flow interface for IMReSQ-MS. Unfortunately, borax crystal formation at the electrode led to the destruction of the interface, **Appendix.** Proving once more, that a more robust interface with a higher dilution factor is required for IMReSQ-MS. To continue experimentation with a sheath-flow interface, a volatile RB must be used.

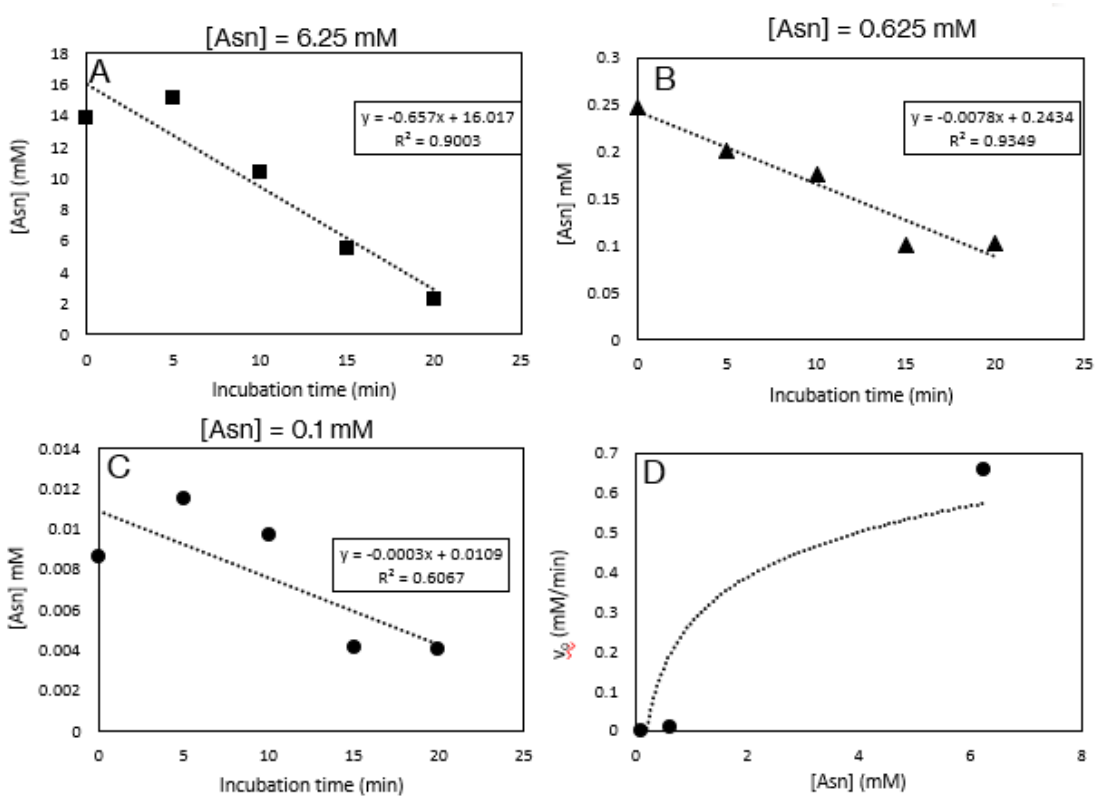

Figure 10: Consumption of Asn by JZP-341 from 0-20 minutes using IMReSQ-MS-(Time-of-Flight). Ion chromatogram peak areas were normalized to internal standard peak area. A= 6.25 mM Asn, B= 0.625 mM Asn, C=0.1 mM Asn D: Michaelis-Menten curve for JZP-341.

Instead, we linked a CE instrument to a TripleTOF mass spectrometer with a prototype OPI. We demonstrated that OPI is compatible with borax as there is significant dilution of the RB with a volatile SL. We tested IMReSQ-MS for JZP-341 at three concentrations of substrate: 6.25 mM Asn, 1 mM Asn, and 0.1 mM Asn, **Figure 10A, B, and C**, respectively. We used borax as our RB and EB, and 25 mM Lys as our internal standard. We observed consumption of Asn in all three

cases with V_o of -0.657 mM Asn/min, -0.0078 mM Asn/min, and -0.0003 mM Asn/min, respectively. **Figure 10D** depicts the dependence of [Asn] on V_o. We observed a hyperbolic relationship that should be further improved with replication and acquiring more data points between 6.25 mM and 20 μM. To test concentrations below 0.1 mM, we should implement a modern triple quadrupole MS/MS which provides better sensitivity for small molecules such as Asn and Asp.

4.8 Conclusions and Future Work

We have demonstrated the preliminary work required for developing a robust enzyme activity for the assessment of JZP-341. We investigated the applicability of fluorescent labelling of the substrate and product. We conclude that fluorescent tags are inefficient and provide weak sensitivity for development of a robust enzyme assay. Instead, we deem mass spectrometry suitable for high sensitivity detection of Asn and Asp. We then optimized IMReSQ-UV parameters so that we can observe and resolve Asn, Asp, and two internal standards with buffer match and buffer mismatch systems. IMReSQ is successful in both buffer-match and buffer-mismatch systems. However, we conclude that UV is not sensitive enough to test for enzyme activity accurately. Also, IMReSQ-MS with SFI is incompatible with the buffer system optimized in IMReSQ-UV experiments, due to the formation of borax crystals. Yet, IMReSQ-MS with OPI is successful at analyzing JZP-341 activity. The OPI significantly dilutes capillary flow which means many different CE buffer systems can be tolerated. The accuracy of detection can be improved by using a modern triple quadrupole detector, which is better suited at analyzing small molecules, instead of a time-of flight mass spectrometer. Ultimately, IMReSQ-MS with OPI has the potential to be a practical and universal enzyme activity assay, where EB, RB, and sheath liquid are all optimized to suit the particular substrate enzyme of interest.

Limitations

Many CE techniques were used in this project with conventional optical detection. Although, optical detection is sufficient for other applications such as studying binding parameters and separating molecules, it is insufficient at providing the high-resolution data required for drug approval. As a result CE with MS detection is required to better understand the effect of the PAS tail on JZP-341. However, as described above, combining CE with MS is not an easy feat. Special consideration must be taken for the type of interface and the buffer systems implemented.

CE is also inherently limited by the injection volume as a typical capillary can only hold just under 1 μL. As a result, CE cannot be used to collect fractions of non-amplifiable molecules, such as proteins. Again, we can circumvent this by directly connecting the CE to an MS with minimal dilution at the interface so that the analytes can be analyzed directly.

Conclusions and Future Work

In this report, we describe the use of CZE and CGE to study structural heterogeneity, cIEF to study charge heterogeneity; and HPLC, CZE, and CE-MS to study enzyme activity. We learned that JZP-341 has some structural and charge heterogeneity, but could not determine exactly what is the cause of the heterogeneity. If we combine CZE and CGE with MS we have the potential to identify the different structural conformers. In particular, a successful native-CGE-MS assay can be used to validate many pre-clinical protein drugs and fast-track the approval of bio-betters. More sophisticated HDX-MS, IMR, and 2D-NMR fingerprinting should be implemented orthogonally to corroborate the results. cIEF-MS with an OPI can aid in identifying the charge variants and elucidating the associated PTMs. The OPI can significantly dilute the ampholytes used in cIEF making it compatible with MS.

We conclude that enzyme activity is best studied with a label-free, automated, and sensitive IMReSQ-MS. We confirmed that JZP-341 is active and we can monitor its activity using IMReSQ-MS. Future work should include establishing IMReSQ-MS as a universal enzymatic assay, as the OPI grants the freedom to use almost any buffer to optimize the enzymatic reaction, separation, and ionization. Other universal enzymatic assays suffer from large reagent volume requirements, inaccuracy, require pure samples, and lack of automation.[52,53] An IMReSQ-MS universal enzymatic assay would overcome the aforementioned limitations, and can be used to compare the efficacy and potency of different enzyme drugs at any stage in production. Once established, CZE-MS, native-CGE-MS, cIEF-MS, and IMReSQ-MS experiments should be used to test other lots of JZP-341 and Rylaze for comparability testing.

References

(1) Datta-Mannan, A. Mechanisms Influencing the Pharmacokinetics and Disposition of Monoclonal Antibodies and Peptides. *Drug Metab. Dispos.* **2019**, *47* (10), 1100–1110. https://doi.org/10.1124/DMD.119.086488.

(2) Hamuro, L. L.; Kishnani, N. S. Metabolism of Biologics: Biotherapeutic Proteins. *Bioanalysis* **2012**, *4* (2), 189–195. https://doi.org/10.4155/BIO.11.304.

(3) Cohen, B. A.; Rieckmann, P. Emerging Oral Therapies for Multiple Sclerosis. *Int. J. Clin. Pract.* **2007**, *61* (11), 1922–1930. https://doi.org/10.1111/J.1742-1241.2007.01561..X.

(4) Torres-Obreque, K. M.; Meneguetti, G. P.; Muso-Cachumba, J. J.; Feitosa, V. A.; Santos, J. H. P. M.; Ventura, S. P. M.; Rangel-Yagui, C. O. Building Better Biobetters: From Fundamentals to Industrial Application. *Drug Discov. Today* **2022**, *27* (1), 65–81. https://doi.org/10.1016/J.DRUDIS.2021.08.009.

(5) Wronkowitz, N.; Hartmann, T.; Görgens, S. W.; Dietze-Schroeder, D.; Indrakusuma, I.; Choi, I. Y.; Park, S. H.; Lee, Y. M.; Kwon, S. C.; Kang, Y.; Hompesch, M.; Eckel, J. LAPSInsulin115: A Novel Ultra-Long-Acting Basal Insulin with a Unique Action Profile. *Diabetes, Obes. Metab.* **2017**, *19* (12), 1722–1731. https://doi.org/10.1111/DOM.13006.

(6) van Witteloostuijn, S. B.; Pedersen, S. L.; Jensen, K. J. Half-Life Extension of Biopharmaceuticals Using Chemical Methods: Alternatives to PEGylation. *ChemMedChem* **2016**, *11* (22), 2474–2495. https://doi.org/10.1002/CMDC.201600374.

(7) Gebauer, M.; Skerra, A. Prospects of PASylation® for the Design of Protein and Peptide Therapeutics with Extended Half-Life and Enhanced Action. *Bioorg. Med. Chem.* **2018**, *26* (10), 2882–2887. https://doi.org/10.1016/J.BMC.2017.09.016.

(8) Torres-Obreque, K. M.; Meneguetti, G. P.; Muso-Cachumba, J. J.; Feitosa, V. A.; Santos, J. H. P. M.; Ventura, S. P. M.; Rangel-Yagui, C. O. Building Better Biobetters: From Fundamentals to Industrial Application. *Drug Discov. Today* **2022**, *27* (1), 65–81. https://doi.org/10.1016/J.DRUDIS.2021.08.009.

(9) Schlapschy, M.; Binder, U.; Börger, C.; Theobald, I.; Wachinger, K.; Kisling, S.; Haller, D.; Skerra, A. PASylation: A Biological Alternative to PEGylation for Extending theplasma Half-Life of Pharmaceutically Active Proteins. *Protein Eng. Des. Sel.* **2013**, *26* (8), 489. https://doi.org/10.1093/PROTEIN/GZT023.

(10) Binder, U.; Skerra, A. PASylation®: A Versatile Technology to Extend Drug Delivery. *Curr. Opin. Colloid Interface Sci.* **2017**, *31*, 10–17. https://doi.org/10.1016/J.COCIS.2017.06.004.

(11) Breibeck, J.; Skerra, A. The Polypeptide Biophysics of Proline/Alanine-Rich Sequences (PAS): Recombinant Biopolymers with PEG-like Properties. *Biopolymers* **2018**, *109* (1), e23069. https://doi.org/10.1002/BIP.23069.

(12) Richter, A.; Knorr, K.; Schlapschy, M.; Robu, S.; Morath, V.; Mendler, C.; Yen, H. Y.; Steiger, K.; Kiechle, M.; Weber, W.; Skerra, A.; Schwaiger, M. First In-Human Medical Imaging with a PASylated 89Zr-Labeled Anti-HER2 Fab-Fragment in a Patient with Metastatic Breast Cancer. *Nucl. Med. Mol. Imaging (2010).* **2020**, *54* (2), 114–119. https://doi.org/10.1007/S13139-020-00638-7.

(13) Breibeck, J.; Skerra, A. The Polypeptide Biophysics of Proline/Alanine-Rich Sequences (PAS): Recombinant Biopolymers with PEG-like Properties. *Biopolymers* **2018**, *109* (1). https://doi.org/10.1002/bip.23069.

(14) Katz, A. J.; Chia, V. M.; Schoonen, W. M.; Kelsh, M. A. Acute Lymphoblastic Leukemia: An Assessment of International Incidence, Survival, and Disease Burden. *Cancer Causes Control* **2015**, *26* (11), 1627–1642. https://doi.org/10.1007/S10552-015-0657-6/TABLES/5.

(15) Katz, A. J.; Chia, V. M.; Schoonen, W. M.; Kelsh, M. A. Acute Lymphoblastic Leukemia: An Assessment of International Incidence, Survival, and Disease Burden. *Cancer Causes Control* **2015**, *26* (11), 1627–1642. https://doi.org/10.1007/S10552-015-0657-6/TABLES/5.

(16) Broome, J. D. Evidence That the L-Asparaginase Activity of Guinea Pig Serum Is Responsible for Its Antilymphoma Effects. *Nature* **1961**, *191* (4793), 1114–1115. https://doi.org/10.1038/1911114a0.

(17) Salzer, W. L.; Asselin, B. L.; Plourde, P. V.; Corn, T.; Hunger, S. P. Development of Asparaginase Erwinia Chrysanthemi for the Treatment of Acute Lymphoblastic Leukemia. *Ann. N. Y. Acad. Sci.* **2014**, *1329* (1), 81–92. https://doi.org/10.1111/NYAS.12496.

(18) Chiu, M.; Taurino, G.; Bianchi, M. G.; Kilberg, M. S.; Bussolati, O. Asparagine Synthetase in Cancer: Beyond Acute Lymphoblastic Leukemia. *Front. Oncol.* **2020**, *9*, 1480. https://doi.org/10.3389/FONC.2019.01480/BIBTEX.

(19) Maese, L.; Rizzari, C.; Coleman, R.; Power, A.; van der Sluis, I.; Rau, R. E. Can Recombinant Technology Address Asparaginase Erwinia Chrysanthemi Shortages? *Pediatr. Blood Cancer* **2021**, *68* (10). https://doi.org/10.1002/pbc.29169.

(20) Ewing, A. G.; Wallingford, R. A.; Olefirowicz, T. M. CAPILLARY ELECTROPHORESIS. *Anal. Chem.* **2012**, *61* (4), 292A-303A. https://doi.org/10.1021/AC00179A722.

(21) Rathore, A. S.; Horváth, C. Capillary Electrochromatography: Theories on Electroosmotic Flow in Porous Media. *J. Chromatogr. A* **1997**, *781* (1–2), 185–195. https://doi.org/10.1016/S0021-9673(97)00627-4.

(22) Lee, C. S.; Blanchard, W. C.; Wu1, C.-T. Direct Control of the Electroosmosis in Capillary Zone Electrophoresis by Using an External Electric Field. *Anal. Chem* **1990**, *62*, 1550–1552.

(23) Monnig, C. A.; Kennedy, R. T. Capillary Electrophoresis. *Anal. Chem* **1994**, 66–280.

(24) Cole, R. B. Electrospray and MALDI Mass Spectrometry : Fundamentals, Instrumentation, Practicalities, and Biological Applications. **2010**, 847.

(25) Banerjee, S.; Mazumdar, S. Electrospray Ionization Mass Spectrometry: A Technique to Access the Information beyond the Molecular Weight of the Analyte. *Int. J. Anal. Chem.* **2012**, *2012*, 1–40. https://doi.org/10.1155/2012/282574.

(26) F.R.S., L. R. XX. On the Equilibrium of Liquid Conducting Masses Charged with Electricity. *London, Edinburgh, Dublin Philos. Mag. J. Sci.* **1882**, *14* (87), 184–186. https://doi.org/10.1080/14786448208628425.

(27) Taylor, G. I.; Mcewan, A. D. The Stability of a Horizontal Fluid Interface in a Vertical Electric Field. *J. Fluid Mech.* **1965**, *22* (1), 1–15. https://doi.org/10.1017/S0022112065000538.

(28) Chernushevich, I. V.; Loboda, A. V.; Thomson, B. A. An Introduction to Quadrupole-Time-of-Flight Mass Spectrometry. *J. Mass Spectrom.* **2001**, *36* (8), 849–865. https://doi.org/10.1002/JMS.207.

(29) Drabovich, A. P.; Berezovski, M.; Okhonin, V.; Krylov, S. N. Selection of Smart Aptamers by Methods of Kinetic Capillary Electrophoresis. *Anal. Chem.* **2006**, *78* (9), 3171–3178.

https://doi.org/10.1021/AC060144H.

(30) Guttman, A.; Filep, C.; Karger, B. L. Fundamentals of Capillary Electrophoretic Migration and Separation of SDS Proteins in Borate Cross-Linked Dextran Gels. *Anal. Chem.* **2021**, *93* (26), 9267–9276. https://doi.org/10.1021/ACS.ANALCHEM.1C01636.

(31) Aebersold, R.; Agar, J. N.; Amster, I. J.; Baker, M. S.; Bertozzi, C. R.; Boja, E. S.; Costello, C. E.; Cravatt, B. F.; Fenselau, C.; Garcia, B. A.; Ge, Y.; Gunawardena, J.; Hendrickson, R. C.; Hergenrother, P. J.; Huber, C. G.; Ivanov, A. R.; Jensen, O. N.; Jewett, M. C.; Kelleher, N. L.; Kiessling, L. L.; Krogan, N. J.; Larsen, M. R.; Loo, J. A.; Ogorzalek Loo, R. R.; Lundberg, E.; Maccoss, M. J.; Mallick, P.; Mootha, V. K.; Mrksich, M.; Muir, T. W.; Patrie, S. M.; Pesavento, J. J.; Pitteri, S. J.; Rodriguez, H.; Saghatelian, A.; Sandoval, W.; Schlüter, H.; Sechi, S.; Slavoff, S. A.; Smith, L. M.; Snyder, M. P.; Thomas, P. M.; Uhlén, M.; Van Eyk, J. E.; Vidal, M.; Walt, D. R.; White, F. M.; Williams, E. R.; Wohlschlager, T.; Wysocki, V. H.; Yates, N. A.; Young, N. L.; Zhang, B. How Many Human Proteoforms Are There? *Nat. Chem. Biol. 2018 143* **2018**, *14* (3), 206–214. https://doi.org/10.1038/nchembio.2576.

(32) Yan, Y.; Liu, A. P.; Wang, S.; Daly, T. J.; Li, N. Ultrasensitive Characterization of Charge Heterogeneity of Therapeutic Monoclonal Antibodies Using Strong Cation Exchange Chromatography Coupled to Native Mass Spectrometry. *Anal. Chem.* **2018**, *90* (21), 13013–13020. https://doi.org/10.1021/ACS.ANALCHEM.8B03773/ASSET/IMAGES/LARGE/AC-2018-03773B_0004.JPEG.

(33) Kumar, R.; Guttman, A.; Rathore, A. S. Applications of Capillary Electrophoresis for Biopharmaceutical Product Characterization. *Electrophoresis* **2022**, *43* (1–2), 143–166. https://doi.org/10.1002/ELPS.202100182.

(34) Gervais, D.; King, D. Capillary Isoelectric Focusing of a Difficult-to-Denature Tetrameric Enzyme Using Alkylurea-Urea Mixtures. *Anal. Biochem.* **2014**, *465*, 90–95. https://doi.org/10.1016/J.AB.2014.08.004.

(35) de la Fuente, M.; Lombardero, L.; Gómez-González, A.; Solari, C.; Angulo-barturen, I.; Acera, A.; Vecino, E.; Astigarraga, E.; Barreda-gómez, G. Enzyme Therapy: Current Challenges and Future Perspectives. *Int. J. Mol. Sci. 2021, Vol. 22, Page 9181* **2021**, *22* (17), 9181. https://doi.org/10.3390/IJMS22179181.

(36) Kirk, O.; Borchert, T. V.; Fuglsang, C. C. Industrial Enzyme Applications. *Curr. Opin. Biotechnol.* **2002**, *13* (4), 345–351. https://doi.org/10.1016/S0958-1669(02)00328-2.

(37) Labrou, N. *Therapeutic Enzymes: Function and Clinical Implications*; 2019; Vol. 1148.

(38) Bisswanger, H. Enzyme Assays. *Perspect. Sci.* **2014**, *1* (1–6), 41–55. https://doi.org/10.1016/J.PISC.2014.02.005.

(39) Bisswanger, H. *Enzyme Kinetics*; Wiley-VCH Verlag GmbH & Co. KGaA: Weinheim, Germany, 2017. https://doi.org/10.1007/978-3-030-11599-9_15.

(40) Choi, B.; Rempala, G. A.; Kim, J. K. Beyond the Michaelis-Menten Equation: Accurate and Efficient Estimation of Enzyme Kinetic Parameters. *Sci. Reports 2017 71* **2017**, *7* (1), 1–11. https://doi.org/10.1038/s41598-017-17072-z.

(41) Kruger, N. J. Errors and Artifacts in Coupled Spectrophotometric Assays of Enzyme Activity. *Phytochemistry* **1995**, *38* (5), 1065–1071. https://doi.org/10.1016/0031-9422(94)00787-T.

(42) Magri, A.; Soler, M. F.; Lopes, A. M.; Cilli, E. M.; Barber, P. S.; Pessoa, A.; Pereira, J. F. B. A Critical Analysis of L-Asparaginase Activity Quantification Methods—Colorimetric Methods

versus High-Performance Liquid Chromatography. *Anal. Bioanal. Chem.* **2018**, *410* (27), 6985–6990. https://doi.org/10.1007/s00216-018-1326-x.

(43) Wong, E.; Okhonin, V.; Berezovski, M. V; Nozaki, T.; Waldmann, H.; Alexandrov, K.; Krylov, S. N. "Inject-Mix-React-Separate-and-Quantitate" (IMReSQ) Method for Screening Enzyme Inhibitors. *J. AM. CHEM. SOC* **2008**, *130*, 11862–11863. https://doi.org/10.1021/ja804544x.

(44) Mironov, G. G.; St-Jacques, A. D.; Mungham, A.; Eason, M. G.; Chica, R. A.; Berezovski, M. V. Bioanalysis for Biocatalysis: Multiplexed Capillary Electrophoresis-Mass Spectrometry Assay for Aminotransferase Substrate Discovery and Specificity Profiling. *J. Am. Chem. Soc.* **2013**, *135* (37), 13728–13736. https://doi.org/10.1021/JA407486Z/SUPPL_FILE/JA407486Z_SI_001.PDF.

(45) Wang, W. F.; Yang, J. L. Advances in Screening Enzyme Inhibitors by Capillary Electrophoresis. *Electrophoresis* **2019**, *40* (16–17), 2075–2083. https://doi.org/10.1002/ELPS.201900013.

(46) Robledo, V. R.; Smyth, W. F. Review of the CE-MS Platform as a Powerful Alternative to Conventional Couplings in Bio-Omics and Target-Based Applications. *Electrophoresis* **2014**, *35* (16), 2292–2308. https://doi.org/10.1002/ELPS.201300561.

(47) Ramautar, R.; Heemskerk, A. A. M.; Hensbergen, P. J.; Deelder, A. M.; Busnel, J. M.; Mayboroda, O. A. CE–MS for Proteomics: Advances in Interface Development and Application. *J. Proteomics* **2012**, *75* (13), 3814–3828. https://doi.org/10.1016/J.JPROT.2012.04.050.

(48) Liu, C. C.; Alary, J. F.; Vollmerhaus, P.; Kadkhodayan, M. Design, Optimisation, and Evaluation of a Sheath Flow Interface for Automated Capillary Electrophoresis-Electrospray-Mass Spectrometry. *Electrophoresis* **2005**, *26* (7–8), 1366–1375. https://doi.org/10.1002/ELPS.200410133.

(49) Van Berkel, G. J.; Kertesz, V. An Open Port Sampling Interface for Liquid Introduction Atmospheric Pressure Ionization Mass Spectrometry. *Rapid Commun. Mass Spectrom.* **2015**, *29* (19), 1749–1756. https://doi.org/10.1002/RCM.7274.

(50) Li, X. F.; Ren, H. J.; Le, X. C.; Qi, M.; Ireland, I. D.; Dovichi, N. J. Migration Time Correction for the Analysis of Derivatized Amino Acids and Oligosaccharides by Micellar Capillary Electrochromatography. *J. Chromatogr. A* **2000**, *869* (1–2), 375–384. https://doi.org/10.1016/S0021-9673(99)00893-6.

(51) Petritis, K.; Chaimbault, P.; Elfakir, C.; Dreux, M. Parameter Optimization for the Analysis of Underivatized Protein Amino Acids by Liquid Chromatography and Ionspray Tandem Mass Spectrometry. *J. Chromatogr. A* **2000**, *896* (1–2), 253–263. https://doi.org/10.1016/S0021-9673(00)00582-3.

(52) Di Trani, J. M.; De Cesco, S.; O'Leary, R.; Plescia, J.; Do Nascimento, C. J.; Moitessier, N.; Mittermaier, A. K. Rapid Measurement of Inhibitor Binding Kinetics by Isothermal Titration Calorimetry /631/45/607 /631/1647/2204 /631/92/613 /631/154 /9 Article. *Nat. Commun.* **2018**, *9* (1). https://doi.org/10.1038/s41467-018-03263-3.

(53) Sinclair, I.; Stearns, R.; Pringle, S.; Wingfield, J.; Datwani, S.; Hall, E.; Ghislain, L.; Majlof, L.; Bachman, M. Novel Acoustic Loading of a Mass Spectrometer: Toward Next-Generation High-Throughput MS Screening. *J. Lab. Autom.* **2016**, *21* (1), 19–26. https://doi.org/10.1177/2211068215619124.

Appendix

CGE Conditioning Protocol:

Initial Conditions | LIF Detector Initial Conditions | Time Program

	Time (min)	Event	Value	Duration	Inlet vial	Outlet vial	Summary	Comments
1		Rinse - Pressure	20.0 psi	10.00 min	BI:D1	BO:D1	forward	naoh
2		Rinse - Pressure	20.0 psi	5.00 min	BI:E1	BO:E1	forward	hcl
3		Rinse - Pressure	20.0 psi	2.00 min	BI:F1	BO:F1	forward	ddh2o
4		Rinse - Pressure	20.0 psi	10.00 min	BI:B1	BO:B1	forward	gel r
5	0.00	Separate - Voltage	15.0 KV	10.00 min	BI:C1	BO:C1	5.00 Min ramp, normal polarity, both	gel s
6								

CGE Separation Protocol:

Initial Conditions | LIF Detector Initial Conditions | Time Program

	Time (min)	Event	Value	Duration	Inlet vial	Outlet vial	Summary	Comments
1		Rinse - Pressure	70.0 psi	3.00 min	BI:D1	BO:D1	forward	naoh
2		Rinse - Pressure	70.0 psi	1.00 min	BI:E1	BO:E1	forward	hcl
3		Rinse - Pressure	50.0 psi	1.00 min	BI:F1	BO:F1	forward	ddh2o
4		Rinse - Pressure	70.0 psi	10.00 min	BI:B1	BO:B1	forward	gel r
5		Wait		0.00 min	BI:A1	BO:A1		
6		Wait		0.00 min	BI:A4	BO:A4		
7		Inject - Pressure	0.5 psi	25.0 sec	SI:A1	BO:C1	Override, forward	
8		Wait		0.00 min	BI:B4	BO:B4		
9	0.00	Separate - Voltage	30.0 KV	200.00 min	BI:C1	BO:C1	5.00 Min ramp, reverse polarity, both	gel s
10	5.00	Autozero						
11								

CIEF Conditioning Protocol:

Initial Conditions | UV Detector Initial Conditions | Time Program

	Time (min)	Event	Value	Duration	Inlet vial	Outlet vial	Summary	
1		Rinse - Pressure	50.0 psi	5.00 min	BI:A5	BO:A5	forward	Water Rinse 1
2		Rinse - Pressure	50.0 psi	5.00 min	BI:F6	BO:F6	forward	SLS Rinse
3		Rinse - Pressure	50.0 psi	3.00 min	BI:B5	BO:B5	forward	Water Rinse 2
4	0.00	Separate - Pressure	50.0 psi	3.00 min	BI:C5	BO:C5	forward	Water Rinse 3
5	3.00	Wait		0.00 min	BI:D5	BO:D5		Water dip
6								

CIEF Separation Protocol:

Initial Conditions | UV Detector Initial Conditions | Time Program

	Time (min)	Event	Value	Duration	Inlet vial	Outlet vial	Summary	
1		Rinse - Pressure	50.0 psi	1.00 min	BI:F6	BO:F6	forward	SLS rinse
2		Rinse - Pressure	20.0 psi	3.00 min	BI:F1	BO:F1	forward, In / Out vial inc 10	Water Rinse 1
3		Rinse - Pressure	50.0 psi	2.00 min	BI:B1	BO:B1	forward, In / Out vial inc 10	Water Rinse 2
4		Inject - Pressure	15.0 psi	150.0 sec	SI:A1	BO:B1	Override, forward	Sample Injection
5		Wait		0.00 min	BI:A1	BO:A1	In / Out vial inc 10	Water dip 1
6	0.00	Separate - Voltage	25.0 KV	15.00 min	BI:C1	BO:C1	0.17 Min ramp, normal polarity, In / Out vial inc 10	Focusing step
7	1.00	Autozero						
8	15.10	Wait		0.00 min	BI:C1	BO:A1	In / Out vial inc 10	Water dip 2
9	15.20	Separate - Voltage	30.0 KV	25.00 min	BI:C1	BO:E1	0.17 Min ramp, normal polarity, In / Out vial inc 10	Mobilization step
10	40.20	Stop data						Stop cIEF separation
11	40.30	Rinse - Pressure	50.0 psi	3.00 min	BI:B1	BO:D1	forward, In / Out vial inc 10	Water Rinse 3
12	43.40	Wait		0.00 min	BI:A1	BO:A1	In / Out vial inc 10	Water dip 3
13	43.50	End						Method end
14								

CIEF Shutdown Protocol:

Initial Conditions | UV Detector Initial Conditions | Time Program

	Time (min)	Event	Value	Duration	Inlet vial	Outlet vial	Summary	
1		Rinse - Pressure	50.0 psi	3.00 min	BI:F6	BO:F6	forward	SLS Rinse
2		Wait		0.00 min	BI:C6	BO:C6		Water dip
3		Rinse - Pressure	50.0 psi	10.00 min	BI:E6	BO:E6	forward	Water Rinse
4	0.00	Separate - Pressure	50.0 psi	3.00 min	BI:D6	BO:D6	forward	cIEF gel Rinse
5	3.10	Lamp - Off						Turn off the lamp
6	3.20	Wait		0.00 min	BI:F5	BO:F5		Water dip
7								

IMReSQ Separation Protocol:

Instrument Setup

Initial Conditions | UV Detector Initial Conditions | Time Program

	Time (min)	Event	Value	Duration	Inlet vial	Outlet vial	Summary	
1		Rinse - Pressure	20.0 psi	2.00 min	BI:A1	BO:A1	forward, In / Out vial inc 3	hcl
2		Rinse - Pressure	20.0 psi	2.00 min	BI:B1	BO:A1	forward, In / Out vial inc 3	naoh
3		Rinse - Pressure	20.0 psi	5.00 min	BI:C1	BO:B1	forward, In / Out vial inc 3	buffer
4		Inject - Pressure	0.1 psi	5.0 sec	SI:A1	BO:B2	Override, forward	
5		Wait		0.00 min	BI:A2	BO:B2		
6		Inject - Pressure	0.1 psi	5.0 sec	SI:A2	BO:B2	No override, forward	
7		Wait		0.00 min	BI:B2	BO:B2		
8		Inject - Pressure	0.1 psi	5.0 sec	SI:A1	BO:B2	No override, forward	
9		Wait		0.00 min	BI:C2	BO:B2		
10		Inject - Pressure	0.1 psi	15.0 sec	SI:A3	BO:B2	No override, forward	
11		Wait		30.00 min	BI:D2	BO:B2		
12	0.00	Separate - Voltage	25.0 KV	60.00 min	BI:E1	BO:C1	0.17 Min ramp, normal polarity, In / Out vial inc 3	
13	0.01	Autozero						
14								

Two-Point Migration Time Correction:

We correct for small changes in the surface chemistry of the capillary and differences in injection volume which affect electroosmotic flow and effective capillary length, respectively, by using a 2-point correction method described by the Dovichi lab, [50]

$$\gamma = \frac{\frac{1}{\hat{t}_{m_1}} - \frac{1}{\hat{t}_{m_2}}}{\frac{1}{t_{m_1}} - \frac{1}{t_{m_2}}}$$

$$t_{corrected} = \left[\frac{1}{t_{m_1}} - \frac{1}{\gamma}\left(\frac{1}{\hat{t}_{m_1}} - \frac{1}{\hat{t}_x}\right)\right]^{-1}$$

Where, γ is the fractional change in electrophoretic mobility. t and $\hat{t}$ denotes migration time at standard and non-standard conditions, respectively. Subscripts m1 and m2 denote the two markers, internal standard and Asn, respectively. The subscript x denotes the analyte.[50]

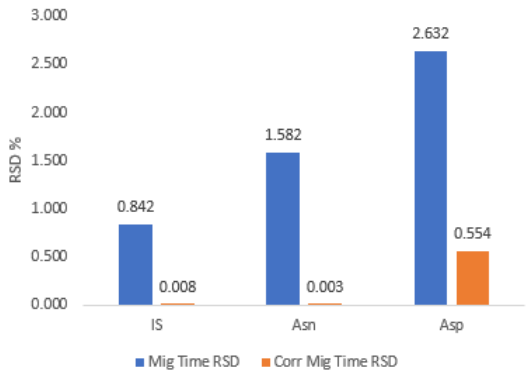

Comparison of relative standard deviation of raw migration time vs. 2-point corrected migration time.

Borax Crystal Formation: